Multifunctional molecular carbon materials—from fullerenes to carbon nanotubes

Dirk M. Guldi, G. M. Aminur Rahman, Vito Sgobba and Christian Ehli

Received 16th January 2006
First published as an Advance Article on the web 6th March 2006
DOI: 10.1039/b511541h

This *critical review* covers the timely topic of carbon nanostructures—fullerenes and carbon nanotubes—in combination with metalloporphyrins as integrative components for *electron-donor–acceptor* ensembles. These ensembles are typically probed in condensed media and at semi-transparent electrode surfaces. In particular, we will present a comprehensive survey of a variety of covalent (*i.e.*, nanoconjugates) and non-covalent linkages (*i.e.*, nanohybrids) to demonstrate how to govern/fine-tune the electronic interactions in the resulting *electron-donor–acceptor* ensembles. In the context of covalent bridges, different spacers will be discussed, which range from pure "insulators" (*i.e.*, amide bonds, *etc.*) to sophisticated "molecular wires" (*i.e.*, *p*-phenylenevinylene units, *etc.*). Furthermore, we will elucidate the fundamental impact that these vastly different spacers may exert on the rate, efficiency, and mechanism of short- and long-range electron transfer reactions. Additionally, a series of non-covalent motifs will be described: *hydrogen bonding, complementary electrostatics, π–π stacking and metal coordination*—to name a few. These motifs have been successfully employed by us and our collaborators *en route* towards novel architectures (*i.e.*, linear structures, tubular structures, rotaxanes, catenanes, *etc.*) that exhibit unique and remarkable charge transfer features.

Universität Erlangen, Institute for Physical and Theoretical Chemistry,
91058 Erlangen, Germany

G. M. Aminur Rahman, Dirk M. Guldi, Vito Sgobba and Christian Ehli

Dirk M. Guldi graduated from the University of Cologne (Germany) in 1988, from where he received his PhD in 1990. In 1992, after a postdoctoral appointment at the National Institute of Standards and Technology, he took a research position at the Hahn-Meitner-Institute Berlin. After a brief stay as a Feodor-Lynen Stipend (Alexander von Humboldt Foundation) at Syracuse University he joined in 1995 the faculty of the Notre Dame Radiation Laboratory where he was promoted to Associate Scientist in 1996. In 1999 he completed his Habilitation at the University of Leipzig (Germany). Since 2004 he has been Professor of Physical Chemistry at the Friedrich-Alexander University in Erlangen (Germany). He was awarded with the Heisenberg-Prize (1999; Deutsche Forschungsgemeinschaft), Grammaticakis-Neumann-Prize (2000; Swiss Society for Photochemistry and Photophysics), JSPS Fellowship (2003; The Japan Society for the Promotion of Science and JPP-Award (2004; Society of Porphyrins and Phthalocyanines). His primary research interests are in the areas of new multifunctional carbon-based nanostructures within the context of light-induced charge separation and solar-energy conversion.

G. M. Aminur Rahman obtained the MSc in Chemistry from the University of Dhaka, Bangladesh in 1996. In 2003, he received his PhD in Organic Chemistry from Niigata University, Japan under the supervision of Prof. T. Akasaka. In the same year, he moved to the Notre Dame Radiation Laboratory as a postdoctoral research assistant. Presently, he is a postdoctoral fellow with Prof. D. M. Guldi, at the Friedrich-Alexander University in Erlangen, Germany. His research interests are synthesis, characterization, and properties of fullerenes, endohedral metallofullerenes, and carbon nanotubes.

Vito Sgobba received his "Laurea" in Chemistry from the University of Bari (Italy) in 2000 under the supervision of Prof. F. Naso and his PhD in Material Engineering from the University of Lecce (Italy) in 2003 with Prof. G. Vasapollo. During his PhD studies he joined Prof. L. De Cola's group at the University of Amsterdam for a Maria Curie Training Fellowship. Presently, he is a postdoctoral fellow with Prof. D. M. Guldi, at the Friedrich-Alexander University in Erlangen Germany. His research interests are: synthesis, characterization, and assembly of hybrid (organic/inorganic) nanostructured materials for novel type of solar cells.

Christian Ehli obtained his diploma in chemistry from the University of Erlangen-Nuernberg (Germany) in 2005. Presently, he is a PhD student with Prof. D. M. Guldi. His research interests are characterization and properties of electron donor acceptor ensembles, carbon nanotubes, fullerene, and porphyrin derivates.

Introduction

The bacterial photosynthetic reaction center provides meaningful incentives for the optimization of charge separation processes in artificial model systems—*nanometer scale structures*.[1] Common to all these systems is a relay of short-range energy/electron transfer reactions, evolving among chlorophyll and quinone moieties.[2] Among many key parameters that govern electron transfer reactions the reorganization energy imposes probably the most far reaching impact. The reorganization energy (λ) is the energy required to structurally reorganize the donor, acceptor and their solvation spheres upon electron transfer.[3] For example, the primary electron transfer processes of photosynthesis are characterized by an extremely small reorganization energy (0.2 eV), attained by the transmembrane protein environment.[4] This aspect is central for achieving the ultrafast charge separation and retarding the energy wasting charge recombination, which is highly exergonic ($-\Delta G_{CR}^\circ = 1.2$ eV).[5]

Nanometer scale structures—fullerenes and carbon nanotubes (CNT)—are the focus of considerable interest because they can be used to test fundamental ideas about the roles of dimensionality and confinement in materials of greatly reduced size.[6]

One cast of active *nanometer scale structures* that we consider are the fullerenes.[7] Since the initial discovery of fullerenes, chemists and physicists worldwide have studied solid state properties ranging from superconductivity and nanostructured devices to endohedral fullerene chemistry. The 3-dimensional, spherical structure of fullerenes, which are made of alternating hexagons (*i.e.*, electron rich) and pentagons (*i.e.*, electron deficient) with diameters starting at 7.8 Å for C_{60}, evoked a lively interest to relate their properties to conventional 2-dimensional π-systems. Their extraordinary electron acceptor properties—predicted theoretically and confirmed experimentally—have resulted in noteworthy advances in the areas of light induced electron transfer chemistry and solar energy conversion. It is mainly the small reorganization energy, which fullerenes exhibit in electron transfer reactions, that is accountable for this noteworthy breakthrough. In particular, ultrafast charge separation together with very slow charge recombination features lead to unprecedented long-lived radical ion pair states formed in high quantum efficiencies.

Original and well-established synthetic methodologies, applied to fullerenes, have produced a wide variety of novel derivatives. In particular, such methodologies allow the chemical functionalization of fullerenes in simple or even sophisticated ways. Based on these methods, the synthesis of relatively complex molecular architectures—tetrads and even hexads—has been accomplished, in which the unique electrochemical and photophysical features of C_{60} have largely been preserved.[8]

The second cast of *nanometer scale structures* is CNT.[9] Of the wide range of nanostructures available, CNT, in general, and single wall carbon nanotubes (SWNT), in particular, stand out as unique materials. In fact, CNT have emerged as a new class of materials with exceptionally high tensile strength,[10] the highest thermal conductivity known[11] and extraordinary field emission properties.[12]

SWNT are 1-dimensional nanostructures. SWNT are hexagon networks of carbon atoms, rolled up to create seamless cylinders, along a chiral vector. While their diameters are typically in the range of nanometers, individually CNT reach lengths of up to 4 cm leading to high aspect ratios. Notably, the conductivity of CNT varies between semiconducting and metallic and depends, in large, on the chiral angle of the tubes and their diameter. They readily accept electrons, which can then be transported under nearly ideal conditions along the axis.

On the other hand, multiple concentric graphene cylinders—multiwall carbon nanotubes (MWNT)—exhibit metallic or semiconducting properties, which depend solely on their outermost shell.[13] On account of the large number of concentric cylindrical graphitic tubes present in MWNT, they are considered even more suitable in *electron-donor–acceptor* ensembles than SWNT. It is notable that, in line with this purely structural assumption, appreciable differences were seen as far as the stabilization of charge separation is concerned.[14]

Due to the unique ability of SWNT to form both metallic and semiconducting species, they represent appealing candidates for key building blocks in the construction of photovoltaic devices.[15] A major setback is, however, that carbon nanotubes are subject to strong, mutual interactions through van der Waals forces and, therefore, yield agglomerates of intimately intertwined long tubes. These cohesive forces account for the poor SWNT dispersibility in most common solvents: They hinder in large their chemical manipulation and, more importantly, the realization of the full potential of SWNT in practical applications. To transfer, however, their outstanding properties from the nanoscale to the macroscale the chemical and physical modification of the SWNT and MWNT surface are essential steps.[16]

All the mentioned *nanometer scale structures*—fullerenes and CNT—are natural electron acceptors. Proof of this concept is obtained mathematically even by qualitative molecular orbital theory. The argument starts from isolated C_2 fragments that are brought together starting from infinite distance. Each fragment has a π and a π^* orbital. As they are brought together to form, for example, a CNT, the two degenerate sets of π and π^* orbitals mix prevalently between themselves and spread in energy. The low-lying end of the π^* orbitals is very stable and readily accept electrons.[17]

Porphyrinoid and especially metalloporphyrinoid systems—with their rich and extensive absorptions throughout the visible region of the solar spectrum—hold particularly great promise as integrative building blocks with increased absorptive cross sections.[18] Over the course of recent years they emanate as light harvesting building blocks in the construction of molecular architectures. Their high electronic excitation energy, typically exceeding 2.0 eV, powers a strongly exergonic electron transfer and intercedes hereby the conversion between light and chemical/electrical energy. Another important feature of porphyrins is their highly delocalized π-electron systems. Such delocalization results—upon an uptake or release of electrons—in minimal structural change upon electron transfer. Rich redox properties render porphyrins and porphyrin analogous as essential components in important biological electron transport systems including photosynthesis and respiration.

One of the major challenges that still lie ahead is to regulate the forces, which will ultimately dictate size and shape in relation to function of the resulting *nanometer scale structures*. Can molecular tailoring of fullerenes and CNT contribute to the induction of new assemblies? To address such issues, we have probed in recent years novel *electron-donor–acceptor* ensembles, in which *nanometer scale structures* constitute the acceptor moiety and biomimetic organization principles—*hydrogen bonding, complementary electrostatics, π-π stacking and metal coordination*—and, thereby, ensuring the hierarchical integration of multiple components into well-ordered arrays. These spontaneous organization principles permit engineering of novel functional *electron-donor–acceptor* (nano)conjugates and (nano)hybrids and, simultaneously, achieve predetermined architectures of controlled sizes and outer-shell structures, with high directionality and selectivity. These *nanometer scale structures* have been successfully utilized to convert photolytically generated radical ion pairs into electrical or chemical energy by constructing integrated artificial photosynthetic assemblies on modified indium-tin-oxide electrodes.

The major thrust of this *Review* is to illustrate the versatility of designing, devising, synthesizing, and testing novel *nanometer scale structures* as *electron-donor–acceptor* ensembles. Our largely interdisciplinary strategy focuses on well-defined molecular architectures: we start with building blocks (*i.e.,* at an atomic and/or molecular scale) that give access to *a priori* design of multifunctional molecular materials and their integration into 2- or 3-dimensional solid *electron-donor–acceptor* ensembles.

General considerations

The Marcus theory of electron transfer treats the rate constants of non-adiabatic intramolecular electron transfer—for both charge separation (k_{CS}) and charge recombination (k_{CR})—as a parabolic dependence on the free energy changes of the reaction ($-\Delta G_{\mathrm{CS}}^{\circ}$ or $-\Delta G_{\mathrm{CR}}^{\circ}$).[19] This treatment provides a valuable guide for controlling and optimizing the efficiency of charge separation *versus* charge recombination. Hereby, the electronic coupling (V) between donor and acceptor states and, foremost, the reorganization energies (λ) regulate the absolute rate constants.

Principally, the rate constant first increases with increasing thermodynamic driving force ($-\Delta G^{\circ} < \lambda$), which is generally referred to as the normal region of the bell-shape relationship. When the driving force becomes of the same magnitude as the reorganization energy ($-\Delta G^{\circ} \sim \lambda$), the reaction rate is maximal and is basically controlled by the magnitude of electronic coupling (V) between the donor and acceptor moiety. Hereby, V relates to the overlap of the donor and acceptor orbitals. Upon passing the thermodynamic maximum ($-\Delta G^{\circ} \sim \lambda$), the highly exothermic region of the parabola ($-\Delta G^{\circ} > \lambda$) is entered, in which an additional increase of the thermodynamic driving force results in an actual slow-down of the reaction rate. Primarily, an increasingly poor vibrational overlap of the product and reactant wave functions is responsible for this behavior. The highly exergonic range is generally referred to as the Marcus inverted region.

The ultimate goal is to power a thermodynamically driven charge separation event and yield a highly energetic radical ion pair. In this context, charge separation and, thereby, recovery of most of the excited state energy, should, if conceivable, take place at small free energy changes, $-\Delta G_{\mathrm{CS}}^{\circ}$. The energy gap characterizing the charge recombination ($-\Delta G_{\mathrm{CR}}^{\circ}$), on the other hand, should be kept as large as feasible. Ideally, large energy gaps should ensure dynamics that are deeply shifted into the inverted region and, consequently, to slow down the limiting and energy wasting charge recombination.[20]

Variation of the reorganization energy (λ) is an effective way to modulate the electron transfer rates. In general, modifying λ influences the maximum of the parabolic $\log k_{\mathrm{ET}}$ *vs* $-\Delta G_{\mathrm{ET}}^{\circ}$ dependence on the abscissa. An even more dramatic impact is seen on the activation energies for the charge separation ($\Delta G_{\mathrm{CS}}^{\#}$) and the reverse charge recombination ($\Delta G_{\mathrm{CR}}^{\#}$) are much reduced and increased, respectively. Thus, under optimal conditions, small reorganization energies lead to optimal charge separation kinetics, which are located near the top of the Marcus curve—even if the driving forces are small—and a deceleration of the charge recombination rates, which are shifted far into the inverted region.

The major conclusion of our considerations is that both donor and acceptor moieties should support the stabilization of charges—electrons or holes—within their chemical structures. Delocalization of charges, for example, over a large and extended π-system is unquestionably a very valuable approach to ensure small reorganization energies (λ).

Covalently linked conjugates—fullerenes

3-Dimensional *versus* 2-dimensional

Structural assumptions, as they were discussed above, were clearly confirmed in a comprehensive assay of reorganization energies for inter- and intramolecular electron transfer reactions comparing a 3-dimensional electron acceptor—spherical C_{60}—with a 2-dimensional acceptor—planar naphthalenediimide.[21] This comparison took earlier work on a quinone acceptor (*i.e.*, 2-dimensional) further, where a significant mismatch in driving force for the electron transfer rendered a meaningful interpretation somewhat inconclusive.[22] Our study clearly inferred that intermolecular electron transfer between the planar naphthalenediimide and a planar zinc tetraphenylporphyrin (ZnP) donor takes place at short separation distances rendering the reorganization energy small.[21] In contrast to such a 2-dimensional π-system, intermolecular electron transfer involving a spherical 3-dimensional π-system (C_{60}) is likely to occur at larger distances. An important asset is the effective radius of the acceptor moiety: even if C_{60} is held at the same critical distance (*i.e.*, van der Waals contact) as naphthalenediimide, due to the strong π–π interactions, the effective center-to-center separation is significantly larger. In the case of intramolecular electron transfer systems, the fixed distance, by which the donor and acceptor are separated, allows one to distinguish the intrinsic reorganization energies (λ) and electronic coupling element (V) of a planar and a spherical acceptor. In fact, the λ and V values obtained for the ZnP-C_{60} conjugate from the intercept and the slope are $\lambda = 0.59 \pm 0.15$ eV and $V = 7.9 \pm 1.7$ cm^{-1}, respectively. Although a linear correlation was also obtained for the analogous naphthalenediimide conjugate, much larger λ values ($\lambda = 1.41 \pm 0.33$ eV)—together with a similar V value (7.8 ± 3.2 cm^{-1})—were determined. This study has provided for the first time valuable insights on the intrinsic reorganization energies of electron transfer, as they relate to different molecular shapes.

Bridges

The bridge connecting electron acceptor with electron donor is considered to be vital in the light of several key aspects.[23,24] Firstly, a covalent bridge eliminates diffusion as the rate determining electron transfer step and, thereby, helps enhancement of the transfer dynamics in *electron-donor–acceptor* conjugates. Secondly, the bridge assists in the control over the separation, orientation, overlap and topology in *electron-donor–acceptor* ensembles. Implicit here is that the linking unit must be structurally rigid, thereby preventing unrestrained and unwanted structural rearrangements. Structural flexibility, on the other hand, may result in different photoreactivites (*i.e.*, rates, pathways, products), *etc*. Thirdly, the nature of the bridge influences rates of conductance/charge transport. Finally, the bridge is not expected to affect the electronic nature of the donor–acceptor pair, where the coupling is proportional to the overlap of their electronic clouds.

Scheme 2 illustrates a few leading examples, in which ZnP and C_{60} are held together by diverse bridges.[21] These comprise either i) a –CO–NH– amide bond (in THF, k_{CS}: 2.2×10^{10} s^{-1}; k_{CR}: 2.0×10^{6} s^{-1}), ii) a –NH–CO– reversed amide bond (in THF, k_{CS}: 1.7×10^{10} s^{-1}; k_{CR}: 3.7×10^{5} s^{-1}), iii) a –CC– triple bond (in THF, k_{CS}: 3.7×10^{10} s^{-1}; k_{CR}: 1.5×10^{6} s^{-1}) or iv) a –N=N– double bond (in THF, k_{CS}: 7.2×10^{9} s^{-1}; k_{CR}: 6.8×10^{6} s^{-1}). Although the *electron-donor–acceptor* separations are by and large constant in i) to iv), different electronic couplings, as indicated by different charge separation and charge recombination features (*i.e.*, rates, efficiencies, quantum yields, *etc.*) are observed. As a point of reference the π-stacked ZnP-C_{60} conjugate should be considered, where van der Waals contacts result in much faster picosecond dynamics.

Long distance charge transfer

Considering the nature of all the aforementioned *electron-donor–acceptor* conjugates the efficiency of electron transfer decreases exponentially with increasing bridge length. Any long-range electron transfer processes, which are governed in these conjugates by a superexchange mechanism, are typically limited to distances of around 20 Å. At larger distances the electron transfer rate determining electronic coupling is largely

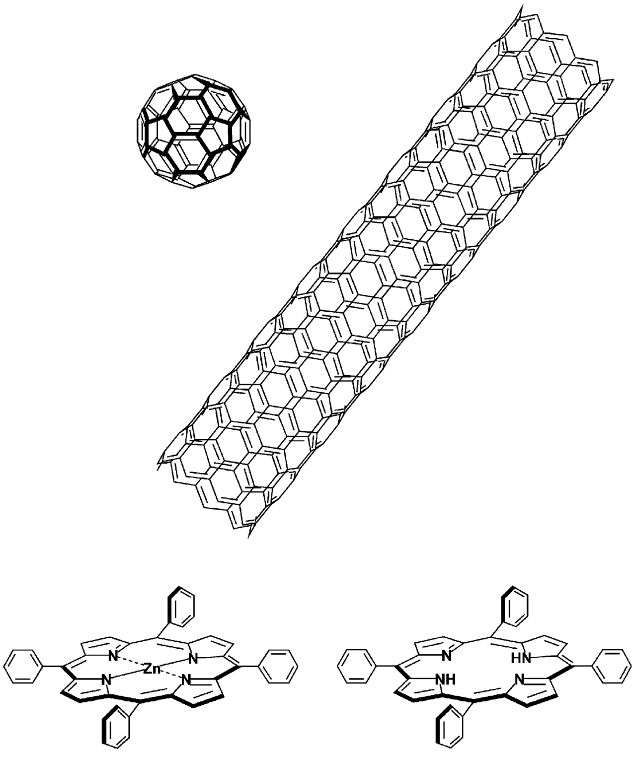

Scheme 1 Molecular building blocks: C_{60}, single wall carbon nanotubes (SWNT), zinc porphyrin (ZnP), and free base porphyrin (H_2P).

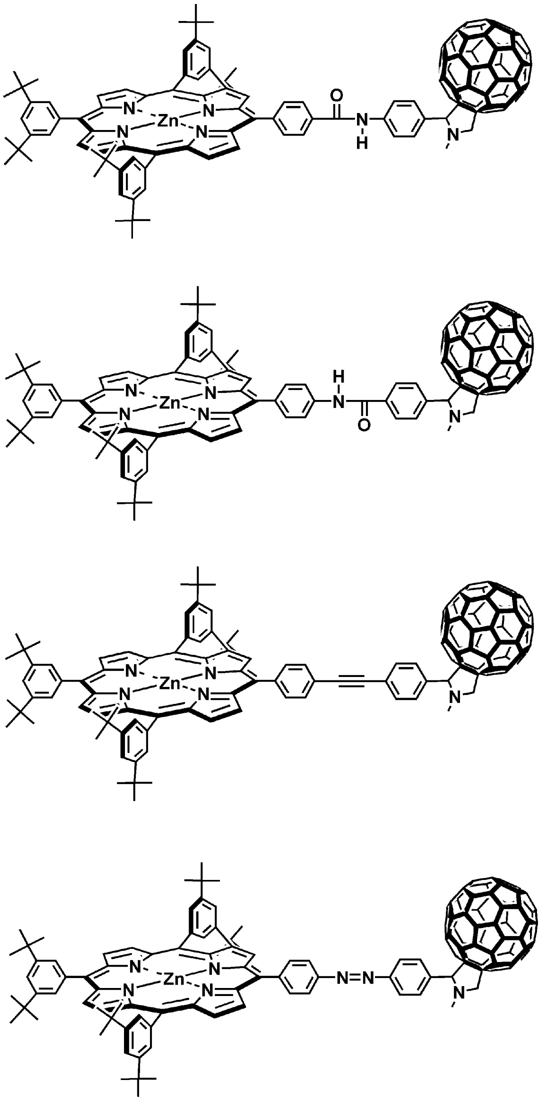

Scheme 2 Leading examples of ZnP-C_{60} conjugates with different spacers: –CO–NH–, –NH–CO–, –CC–, and –N=N–.

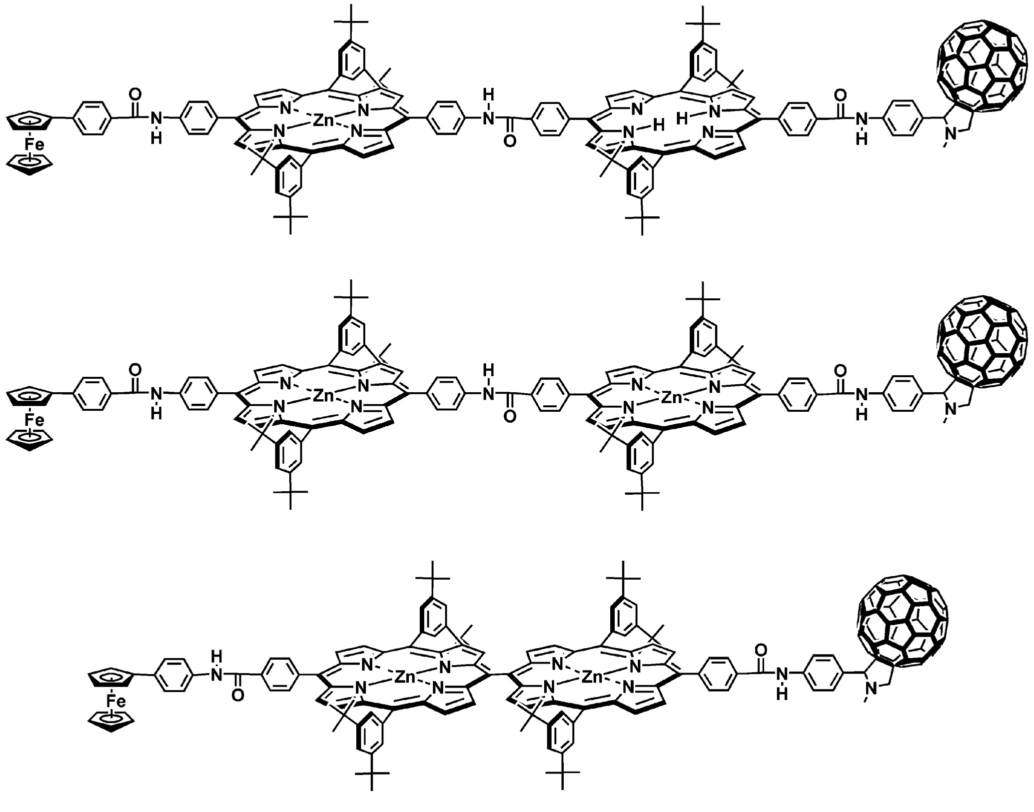

Scheme 3 Leading examples of long distance charge transfer conjugates: Fc-ZnP-H_2P-C_{60}, Fc-ZnP-ZnP-C_{60}, and Fc-$(ZnP)_2$-C_{60}.

diminished and, consequently, is insufficient to compete with the intrinsic deactivation of the excited state electron donor.[25]

Should charges, however, be transported over distances larger than 20 Å alternative concepts have to be applied. This task becomes particularly relevant when achieving ultralong radical ion pair lifetimes. A viable option to achieve long-distance, charge separated states makes use of a relay of several short-range electron transfer steps along well-designed redox gradients rather than forcing the electron transfer through a single, concerted long-range step.

Such a "relay concept" has been successfully realized by combining several redox active building blocks—linking ferrocene (Fc) and ZnP to free base tetraphenylporphyrin (H_2P) and C_{60}—to form Fc-ZnP-H_2P-C_{60} and Fc-ZnP-ZnP-C_{60} conjugates. Scheme 3 summarizes some leading conjugates, where the final electron donors (*i.e.*, Fc) and the primary electron acceptors (*i.e.*, C_{60}) are separated by nearly 50 Å. In these novel molecular examples we demonstrated very slow intramolecular charge recombination processes—observable only by ESR measurements in frozen matrices under light irradiation. When comparing Fc-ZnP-H_2P-C_{60} (0.38 s) or Fc-ZnP-ZnP-C_{60} (1.6 s) conjugates with analogous H_2P-C_{60} or ZnP-C_{60} conjugates the difference in radical ion pair lifetimes amounts to *six orders of magnitude*, that is, seconds *versus* microseconds (!).[26]

Electronic coupling elements are primarily responsible for such outstanding lifetimes that are as small as $(5.6 \pm 0.5) \times 10^{-5}$ cm^{-1} relative to a V value of 7.9 ± 1.7 cm^{-1} seen for the ZnP-C_{60} conjugates, where the *electron-donor–acceptor* separations are ~12 Å.[21] This finding correlates well with negligible

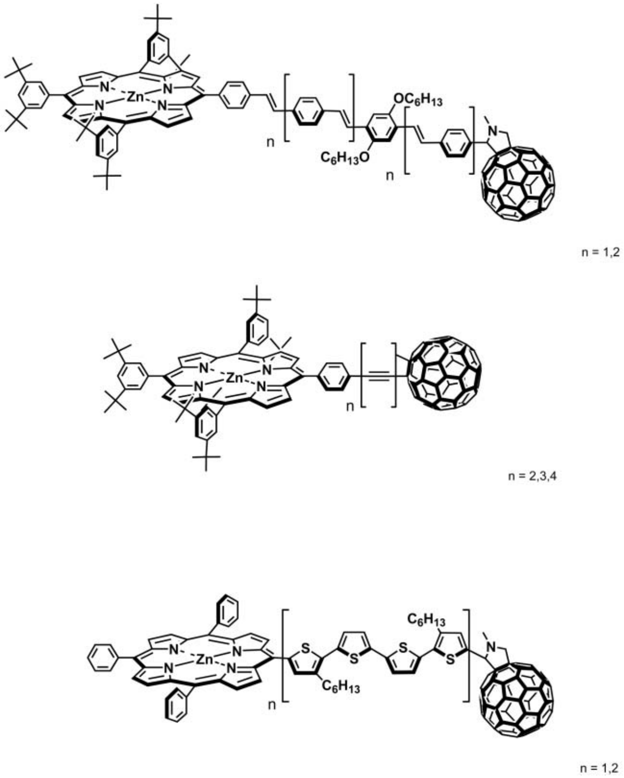

Scheme 4 Leading examples of molecular wire conjugates: ZnP-*p*-phenylenevinylene-C_{60}, ZnP-alkyne-C_{60} and ZnP-thiophene-C_{60}.

orbital overlap—an argument that finds further support when calculating the attenuation factor (β). The attenuation factor describes the intrinsic electronic properties of the bridge, which is related to the distance dependence of electron transfer rate constants. A plot of the radical ion pair lifetimes of Fc-ZnP-H_2P-C_{60} ($\sim$50 Å), ZnP-H_2P-C_{60} ($\sim$30 Å) and H_2P-C_{60} ($\sim$12 Å) *versus electron-donor–acceptor* separation is well fitted with a straight line and yields a β value of 0.60 $Å^{-1}$.[26] Importantly, this β value is located within the boundaries of non-adiabatic electron transfer reactions for saturated hydrocarbon bridges (0.8–1.0 $Å^{-1}$) and unsaturated phenylene bridges (0.4 $Å^{-1}$).[27]

Molecular wires

It is well documented that the attenuation factor is a function of electronic structure and overall architecture of the bridge. Thus, much effort has been devoted to the design of bridges that facilitate long-range electron transfer reactions.[28] In this context, molecular wires that exhibit characteristic paraconjugation are interesting candidates for such an application, since the bridges do not actively participate in the electron transfer events (*i.e.*, charge separation charge recombination, charge hopping, *etc.*). In other words, the molecular wires have only mediating function in transporting charges due to their high-lying LUMO and/or low-lying HOMO.

p-Vinylene[29] and alkyne oligomers[30] are of particular interest as versatile model bridges with chemically tailored properties. Accordingly, we have tested novel series of structurally well-defined *electron-donor–acceptor* conjugates that incorporate ZnP as excited state electron donors and C_{60} as electron acceptors, linked by a number of *p*-phenylenevinylene (ZnP-*p*-phenylenevinylene-C_{60}) or alkyne oligomers (ZnP-alkyne-C_{60}). The following aspects stood hereby at the forefront of our investigations: firstly, a systematic variation of the conjugation length; secondly, determining and evaluating the structural and electronic effects of distance and rates with which charges transfer through *p*-phenylenevinylene or alkyne fragments; finally, testing the molecular-wire behavior in *p*-phenylenevinylene or alkyne based *electron-donor–acceptor* ensembles.

For ZnP-*p*-phenylenevinylene-C_{60}, a detailed physicochemical investigation—testing mainly the long-range charge separation (in THF, $3.9 \pm 0.6 \times 10^9$ s^{-1}) and charge recombination events (in THF, $1.05 \pm 0.15 \times 10^6$ s^{-1}) and kinetics thereof—revealed attenuation factors of 0.03 ± 0.005 $Å^{-1}$.[29] Even relative to unsaturated phenylene bridges (0.4 $Å^{-1}$) these factors are extraordinary small. Important for the wire-like behavior is that the energies of the C_{60}'s HOMOs match specially those of the long *p*-phenylenevinylenes. This facilitates charge injection into the wire. Equally important is the strong electronic coupling, realized through the paraconjugation in *p*-phenylenevinylene. This leads to *electron-donor–acceptor* coupling constants of $\sim$2.0 cm^{-1}—even at *electron-donor–acceptor* separations of 40 $Å^{-1}$—and assists charge transfer reactions that reveal shallow distance dependencies. Remarkable is the fact that these features are realized despite the rotational freedom of the donor–bridge and bridge–acceptor contacts.

Somewhat larger are, however, the attenuation factors (*i.e.*, 0.06 ± 0.005 $Å^{-1}$) found for polyalkyne bridges in ZnP-alkyne-C_{60} with charge separation and charge recombination in the range of $7.5 \pm 2.4 \times 10^9$ s^{-1} and $1.6 \pm 0.2 \times 10^6$ s^{-1}, respectively.[30] Still, our finding proves that even triple bonds are effective mediators of long-range electronic interactions up to nearly—but not limited to—24 Å. An interesting aspect of this work was that the direct linkages between the polyalkynes and C_{60} provide much improved bridge–acceptor contacts.

Common to the aforementioned *electron-donor–acceptor* conjugates is that in temperature dependent measurements the charge recombination kinetics imply an efficient decoupling of the donor–bridge and bridge–acceptor contacts, which leads to a significant slow-down of the electron transfer rates. Reversible interruption of the π-conjugation through a temperature-induced rotation along the wire axis is thought to be responsible for this effect.[29]

An intriguing challenge lies in the incorporation of oligomeric bridges in which the π-conjugation is broken off irreversibly through, for example, the chemical nature of the oligomer. Chiral binaphthyl derivatives meet such criteria.[31] They have also been used as electroactive species and, in contrast, to π-conjugated *p*-phenylenevinylene oligomers, the π-conjugation between the two naphthyl units is efficiently disrupted *via* atropisomerism. Consequently, distances and electronic interactions between donor and C_{60} are drastically changed. In fact, we have found that topological effects of the geometrically well-defined chiral binaphthyl spacer play a leading role in electronic interactions in *electron-donor–acceptor* ensembles. Thus, in ZnP-binaphthyl-C_{60} (Scheme 5), associative π–π interactions augmented by charge transfer interactions favor a conformer in which the ZnP is close to C_{60}, resulting in appreciable through-space electronic communication with charge recombination dynamics of $\sim 10^6$ s^{-1}.[32]

Quite different is the photoreactivity of ZnP-thiophene-C_{60}, because the good electron donor ability of polythiophene oligomers forces these bridges to participate more actively in the charge transfer/transport processes.[33]

Redox-active metal complexes

An appealing variation—relative to previous work that focused on the integration of free base porphyrins (H_2P) or the corresponding zinc analogous (ZnP)—involves the use of metalloporphyrins that bear redox-active metal species. Implementation of two redox centers, *i.e.* the metal and the macrocycle, brings about questions regarding the stabilization gained by localizing the positive charge on the metal center as

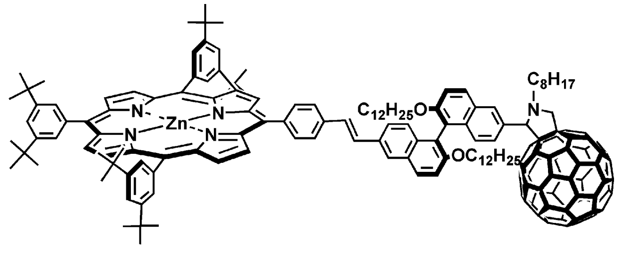

Scheme 5 ZnP-binaphthyl-C_{60} conjugate.

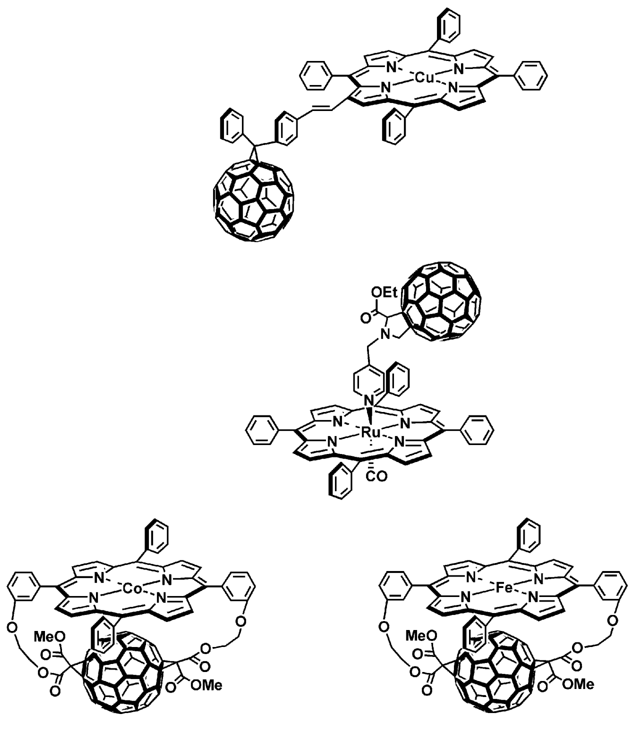

Scheme 6 Leading examples of redox-active metal conjugates: Cu(II)P-C_{60}, Ru(II)P-C_{60}, Co(II)P-C_{60} and Fe(II)P-C_{60}.

compared to the delocalization on the macrocyclic ring. When working, however, with metalloporphyrins—coordinating redox-active transition metals—as electron donors, much impacted excited state lifetimes should govern design considerations.

In, for example, Cu(II)metalloporphyrins (Cu(II)P) thermally equilibrated and long-lived triplet–doublet/triplet–quartet states are a sufficient base for powering intramolecular transfer events. Although the paramagnetic Cu(II) augments the electronic coupling with the electron accepting fullerene and, in turn, influences the charge transfer process, the basic reactivity of photoexcited Cu(II)P-C_{60}, that is, energy transfer in non-polar toluene and electron transfer to form Cu(II)$P^{\bullet+}$-$C_{60}^{\bullet-}$ in polar media, does not support the possibility of forming a Cu(III)P species. The lifetime of the Cu(II)$P^{\bullet+}$-$C_{60}^{\bullet-}$ state is as long as 415 ± 30 ns in chloroform.[34]

An appreciable photoreactivity was also gathered for Ru(II)metalloporphyrins (Ru(II)P), where, nevertheless, an ultrafast/instantaneous intersystem crossing results from the presence of the "heavy-atom" source. The corresponding Ru(II)P-C_{60} conjugates give rise to rapid intramolecular deactivations of the ruthenium porphyrin triplet excited states. The product of the ruthenium porphyrin excited state deactivation depends on the solvent polarity. While in non-polar solvents a transduction of triplet excited energy predominates, in medium and strongly polar media charge-separation leads to the formation of Ru(II)$P^{\bullet+}$-$C_{60}^{\bullet-}$; formation of Ru(III)P-$C_{60}^{\bullet-}$ is ruled out on the basis of spectral analysis.[35]

In contrast to the aforementioned system, a key requirement for testing Co(II) or Fe(III)metalloporphyrins (Co(II)P or Fe(III)P) is a very close *electron-donor–acceptor* separation. This is meant to ensure an ultrafast electron transfer event which allows the utilization of metalloporphyrins that typically deactivate rapidly due to very strong spin orbit coupling. In other words, close van der Waals contacts between electron donor and electron acceptor are a "must". In the case of Co(II)P this was achieved, where significant interactions between the π-system of C_{60} and the d-orbitals of the central atoms were noted.[36] Generally, the short *electron-donor–acceptor* separations guarantee charge separation in any given solvent, from non-polar toluene to polar benzonitrile. A closer look at the charge separation products brings an interesting solvent dependence to light. In toluene, benzonitrile and anisole photoinduced electron transfer leads to the formation of Co(II)$P^{\bullet+}$-$C_{60}^{\bullet-}$ with a lifetime of 560 ± 20 ns in benzonitrile. In contrast, in solvents such as THF, nitrobenzene, *ortho*-diclorobenzene and *tert*-butylbenzene the formation of a Co(III)P-$C_{60}^{\bullet-}$ transient was detected. The latter is, however, short-lived (860 ± 40 ps in THF). Particularly important is the fact that the electronic coupling (V) in Co(III)P-$C_{60}^{\bullet-}$ is with 18 cm^{-1} substantially smaller then the V-value of 313 cm^{-1} in Zn$P^{\bullet+}$-$C_{60}^{\bullet-}$—similar values have to be assumed for Co(II)$P^{\bullet+}$-$C_{60}^{\bullet-}$.[36]

Fe(III)P-C_{60} showed in preliminary tests Fe(III)$P^{\bullet+}$-$C_{60}^{\bullet-}$ as the only appreciable product, whose formation does not depend on the solvent.[37]

Non-covalently linked hybrids—fullerenes

Watson–Crick hydrogen bonding

Recent efforts have been focused on the use of the Watson–Crick hydrogen bonding paradigm—specifically the three-point guanosine–cytidine couple—as a scaffold to assemble molecular *electron-donor–acceptor* hybrids.[38] In particular, studies on a tethered ZnP-cytidine-guanosine-C_{60} hybrid highlight the fact that Watson–Crick base pairing provides a useful means of constructing self-assembled systems, with binding constants of $5.1 \pm 0.5 \times 10^4$ M^{-1} and radical ion pair state lifetimes of 2.02 μs. Although we believe that these natural base-pairs have an important role to play in the generation of functional supramolecular systems, the topology of ZnP-cytidine-guanosine-C_{60} is far from optimum. In particular, through space interactions must be assumed to control charge separation and charge recombination dynamics. This points to the need of a truly linear arrangement in hydrogen bonding *electron-donor–acceptor* hybrids.

Hydrogen bonding

Molecular recognition principles, in the form of crown ether complexation, are the inception for realizing molecularly-organized thin film assemblies and nano-architectures.[39] In this light, ammonium-crown ether recognition and π–π stacking interactions (3.7×10^5 M^{-1}) between H_2P and C_{60} have been employed towards a supramolecular cup-and-ball H_2P-crown-C_{60} hybrid ensemble. Since the emission of the H_2P-crown is fully recovered upon addition of base, which destroys the supramolecular assembly, H_2P-crown-C_{60} appears to be an excellent candidate as a molecular switch operated *via* control of recognition by changing (or adjusting) the pH of the solution.

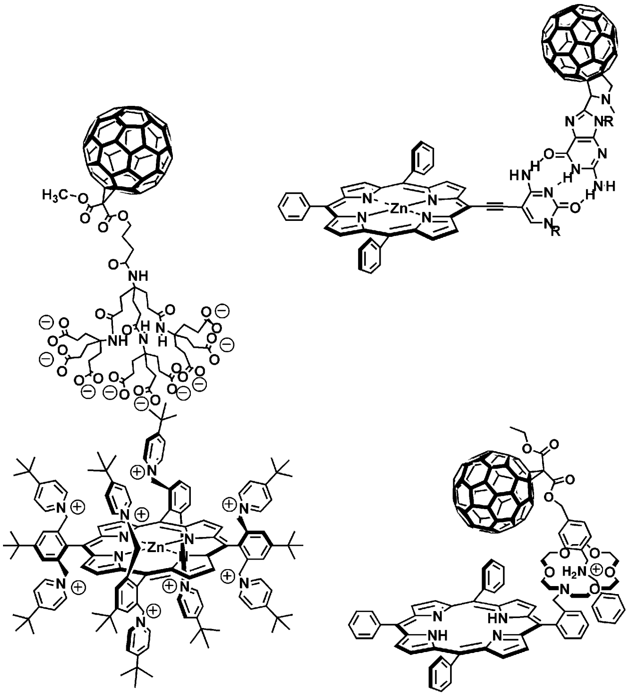

Scheme 7 Leading examples of non-covalently linked hybrids: ZnP-cytidine-guanosine-C_{60}, ZnP-electrostatic-C_{60}, and H_2P-crown-C_{60}.

Complementary electrostatics

More linear is certainly the *electron-donor–acceptor* topology in a coulomb complex comprising a dendritic C_{60} oligocarboxylate and an octapyridinium ZnP salt.[40] A Job plot obtained by monitoring the Soret absorption of the octapyridinium ZnP salt upon addition of the dendritic C_{60} oligocarboxylate in a phosphate buffer (pH 7.2, ionic strength = 0.012) confirmed a 1 : 1 complex—ZnP-electrostatic-C_{60}—for which an association constant of $3.5 \pm 1.0 \times 10^8\ M^{-1}$ was determined. Parallel fluorescence titration experiments revealed that the octapyridinium ZnP salt emission is strongly quenched in the ZnP-electrostatic-C_{60} hybrid. In particular, the noted decrease of fluorescence intensity in the octapyridinium ZnP salt with variation of the dendritic C_{60} oligocarboxylate and evidence for a new, short-lived emissive component suggest a static quenching event inside the ZnP-electrostatic-C_{60} hybrid. From fluorescence titration a value of $1.1 \pm 0.1 \times 10^8\ M^{-1}$ for the association constant of the ZnP-electrostatic-C_{60} hybrid at pH 7.2 was derived. Stability investigations showed the expected disassembly of the complex at higher ionic strength with little dependence on the nature of the anions. Coulomb interactions obviously play a major role in the aggregation process. Electron transfer quenching was confirmed by transient absorption spectroscopy, which showed the fingerprint absorptions of the octapyridinium ZnP salt radical cation and the dendritic C_{60} oligocarboxylate radical anion and a lifetime of 1.1 μs for the charge separated state.

In related work, the same dendritic C_{60} oligocarboxylate was examined with respect to electrostatic complexation with cytochrome *c* (Cyt*c*).[41] The zinc analog of Cyt*c* (ZnCyt*c*), which is necessary for the photophysical investigations, was prepared according to a novel modified procedure. The association of ZnCyt*c* and the dendritic C_{60} oligocarboxylate ($\sim 10^5\ M^{-1}$), and consequential photoinduced electron transfer within ZnCyt*c*-electrostatic-C_{60} from the photoexcited protein to the fullerene, is proven by fluorescence spectroscopy and transient absorption spectroscopy. These findings are in addition supported by circular dichroism as well as by extensive molecular dynamics (MD) simulations.

π–π Interactions

Induction of self-organization between H_2P and C_{60} moieties in an amphiphilic H_2P-C_{60} salt, which occurs predominantly through intermolecular forces, results in uniformly nanostructured 1-dimensional nanotubules.[42] The photoreactivity of such nanotubules was also investigated for the corresponding phthalocyanine (ZnPc), where ultrafast charge separation is combined with ultraslow charge recombination. The observed radical ion pair lifetime of 1.4 ms implies, relative to the monomeric analog ($\tau \sim 3$ ns), an impressive stabilization *of six orders of magnitude*. In fact, the lifetime reaches into a time domain found in thin solid films of *electron-donor–acceptor* ensembles.

Metal coordination

Promising success for realizing *electron-donor–acceptor* hybrids was presented through the reversible coordination of pyridine functionalized fullerene ligands to the square-planar zinc center, which constitutes a labile but, nevertheless, measurable binding motif. However, in most of the known examples metal coordination to C_{60} leads to tilted configurations and through space interactions.[43] In this light, a novel, more linearly aligned supramolecular architecture was assembled, based on linking a heterofullerene acceptor ($C_{59}N$)—bearing a pyridine functionality—to the central zinc atom of ZnP donor. The linear refinement was achieved by attaching the donor pyridine ring to $C_{59}N$. The ZnP-pyridine-$C_{59}N$ adduct ($1.1 \times 10^4\ M^{-1}$) is also ideally suited for devising integrated model systems to transmit and process solar energy. Depending on the solvent either photoinduced singlet–singlet energy transfer or electron-transfer was observed. The latter process takes place in *o*-dichlorobenzene as solvent and leads to the corresponding one-electron reduced $C_{59}N$ π-radical anion and one-electron oxidized ZnP π-radical cation that decay with $6.9 \times 10^6\ s^{-1}$.[44]

In contrast to several previous examples, synthesis of a truly linear non-covalently linked ZnP-pyridine-C_{60} dyad was

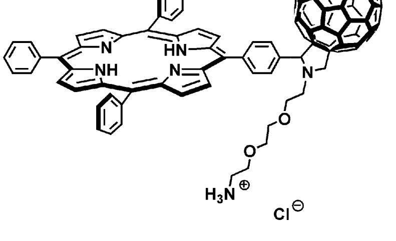

Scheme 8 Amphiphilic H_2P-C_{60} salt.

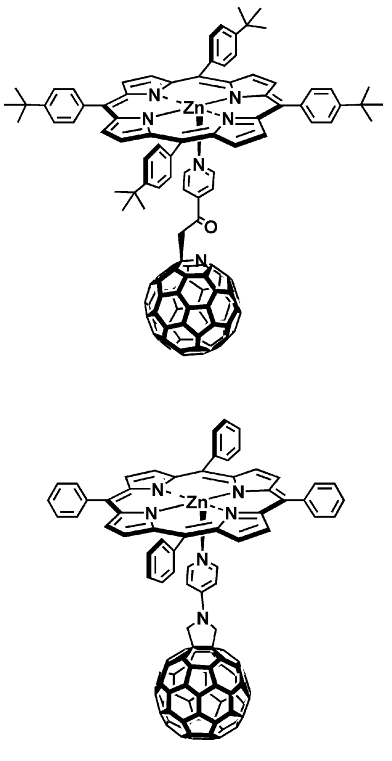

Scheme 9 Leading examples of metal coordination conjugates: ZnP-pyridine-$C_{59}N$ and ZnP-pyridine-C_{60}.

accomplished by attaching the pyridine functionality to the nitrogen of the fulleropyrrolidine. The axially symmetric complexes with ZnP disclose stronger complexation features (7.4×10^4 M^{-1}) than analogous complexes where the pyridine functionality has been linked to a carbon on the pyrrolidine ring (1.4×10^4 M^{-1}).[45]

In an extension of earlier work a novel triad system composed of a zinc porphyrin appended with hydrogen-bonding groups such as either a carboxylic acid or an amide group (ZnP-COOH or ZnP-NH_2) and C_{60} appended with a pyridine group and a *N*,*N*-dimethylaniline (DMA) group acting as a secondary electron donor (C_{60}-DMA). The triad system is self-assembled *via* a "two-point" binding motif, where the pyridine group on the C_{60} axially ligates to the central metal of the zinc porphyrin, while the nitrogen of the fulleropyrrolidine ring hydrogen bonds with the hydrogen-bonding group attached to ZnP, either ZnP-COOH or ZnP-NH_2.[46]

Rotaxanes

Mechanically linked nanoscale ensembles, such as rotaxanes and catenanes, emerged as viable multicomponent model systems to transmit and process solar energy, in large part due to the close resemblance with the topology in the natural photosynthetic reaction center.[47] Two sets of ZnP-rotaxane-C_{60} hybrids have been realized using Sauvage's methodology, that is, threading through a Cu(I)phenanthroline complex, $[Cu(phen)_2]^+$.[48] Because of the tetrahedral arrangement of the phenanthroline ligands around the Cu(I) center, the electron donor (ZnP) and electron acceptor (C_{60}) are separated by nearly 20 Å, which prevents both charge separation and charge recombination processes from occurring directly through space. In other words, the topology of these systems prevents close approach of the ZnP and C_{60} moieties, which was independently confirmed by molecular modeling, so that intramolecular electronic interactions following excitation must take place through the $[Cu(phen)_2]^+$ complex.

In the first set (*i.e.*, ZnP-stoppered hybrids), C_{60} is linked to the macrocycle, while ZnP function as stoppers. Fluorescence and transient absorption spectra indicate that a sequence of energy and electron transfer processes occur along an energy gradient, involving energy transfer from the initially generated porphyrin singlet excited state to the $[Cu(phen)_2]^+$ MLCT state, electron transfer from the excited MLCT state to the C_{60} moiety. Finally, charge transfer from the porphyrin to the oxidized Cu complex, which according to electrochemical data may be reversible, gives the long-distance $(ZnP^{\bullet+})_2$-$[Cu(phen)_2]^+$-$C_{60}^{\bullet-}$ radical ion pair state, which was detected spectroscopically. The measured radical pair lifetimes at room temperature, measured by decay of the absorption due to transient one-electron oxidized ZnP radical cations and the one-electron reduced C_{60} radical anions, are 0.49 and 1.17 μs. The enhanced lifetimes of these nanosized radical ion pair states is attributed to the unique topology of the system.

The lifetimes are also considerably longer than the radical ion pair lifetime of 180 ns observed for a H_2P-rotaxane-C_{60} hybrid loosely held together by just hydrogen bonds. This enhancement in radical ion pair lifetime is consistent with the significant difference in topology in these two supramolecular systems.[49]

In the second set (*i.e.*, C_{60}-stoppered hybrids), the locations of the ZnP and C_{60} moieties are reversed from that described above, that is, the ZnP is appended to the macrocycle and C_{60} moieties are the stoppers on the thread around the central $[Cu(phen)_2]^+$ core. This change in topology results in greatly enhanced lifetimes (0.73 μs) of the $ZnP^{\bullet+}$-$[Cu(phen)_2]^+$-$(C_{60})_2^{\bullet-}$ radical ion pair state produced upon photoexcitation of these materials.

Catenanes

Molecular modeling of ZnP-stoppered ZnP-rotaxane-C_{60} hybrids and the corresponding model rotaxane suggested that the two ZnP linked to the $[Cu(phen)_2]^+$ core constitute a molecular scaffold that should exhibit excellent binding features toward a variety of bidentate guest molecules that coordinate to ZnP. Selective complexation of, for example, the free nitrogen lone pairs of diazabicyclooctane (DABCO) or 4,4′-bipyridyl to the axial d_{z^2} orbitals of ZnP opens pathways to novel photo- and redoxactive catenanic architectures. The latter undergo upon photoexcitation a sequence of short range energy and electron transfer events to give long-lived radical ion pair states with lifetimes of (500 ± 50 ns).[50]

Covalently linked nanoconjugates—carbon nanotubes

First examples of nanoconjugates

An intriguing concept involves using the surface of semiconducting and metallic CNT as intriguing templates to integrate

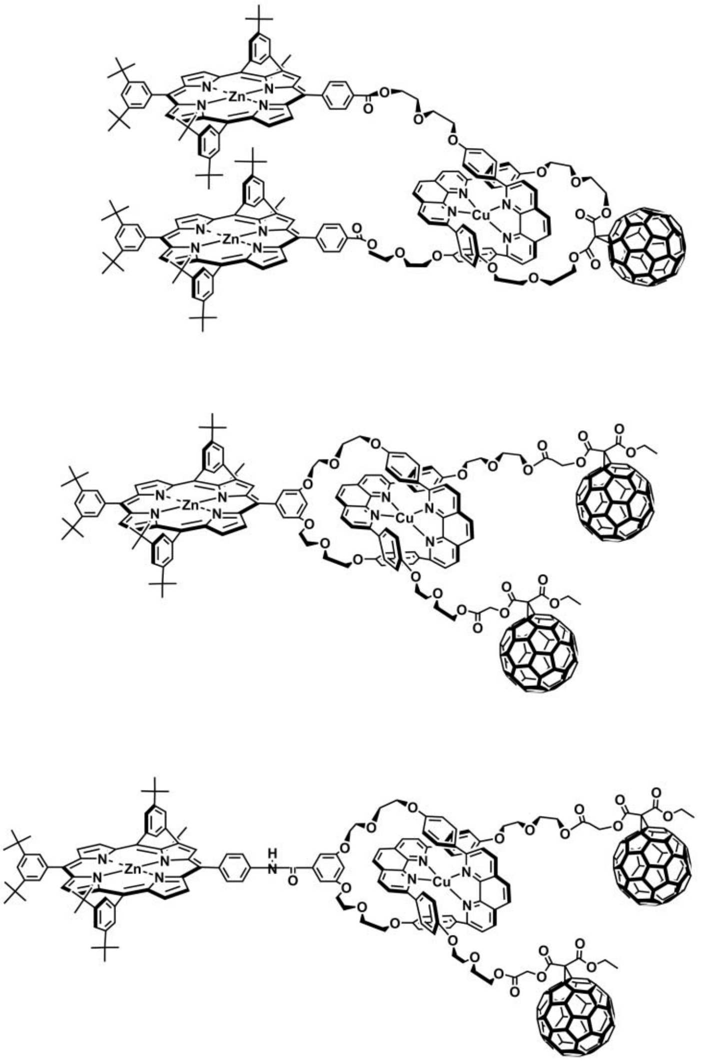

Scheme 10 Leading examples of rotaxanes: ZnP-rotaxane-C_{60} hybrids: $(ZnP)_2$-$[Cu(phen)_2]^+$-C_{60} and ZnP-$[Cu(phen)_2]^+$-$(C_{60})_2$.

porphyrins that serve as visible light harvesting chromophores.[51] For example, the efficient covalent tethering of SWNT with porphyrins was achieved through the esterification of SWNT bound carboxylic acid groups. Based on the initially established approach the surface-bound carboxylic acid groups were produced by acid treatment of CNT. In particular, the work started with two porphyrin derivatives containing terminal hydroxyl groups [5-(*p*-hydroxyhexyloxyphenyl)-10,15,20-tris(*p*-hexadecyloxyphenyl)-21*H*,23*H*-porphine] and [5-(*p*-hydroxymethylphenyl)-10,15,20-tris(*p*-hexadecyloxyphenyl)-21*H*,23*H*-porphine].[52] In the corresponding *electron-donor–acceptor* nanoconjugates (*i.e.*, H_2P-SWNT) the photoexcited porphyrins deactivate, through a transduction of excited state energy. Interestingly, the rates and efficiencies of the excited state transfer depend on the length of the tether that links the porphyrins with the SWNT. Thus, the materials with the shorter tethers showed the least fluorescence quenching.

Subsequently, these carboxylic functionalities proved to be convenient for linking 5-*p*-hydroxyphenyl-10,15,20-tritolylporphyrin to either SWNT or MWNT.[53] According to thermogravimetric analyses (TGA) the amount of grafted porphyrin was estimated to range from 8 to 22%, depending on the initially employed porphyrin concentration.

Non-covalently linked nanohybrids—carbon nanotubes

Polymer wrapping

Recently, we succeeded in the facile supramolecular association of pristine SWNT with linearly polymerized porphyrin polymers towards versatile *electron-donor–acceptor* nanohybrids.[54] The target SWNT nanohybrids, which are dispersable in organic media, were realized through the use of soluble and redox-inert poly(methylmethacrylate) (PMMA) bearing surface immobilized porphyrins (*i.e.*, H_2P-polymer). Conclusive evidence for H_2P-polymer/SWNT interactions came from absorption spectroscopy: The fingerprints of SWNT and H_2P-polymer are discernable throughout the UV, VIS, and NIR part of the spectrum. A similar conclusion was also derived from transmission electron microscopy (TEM) and atomic force microscopy (AFM). AFM images illustrate,

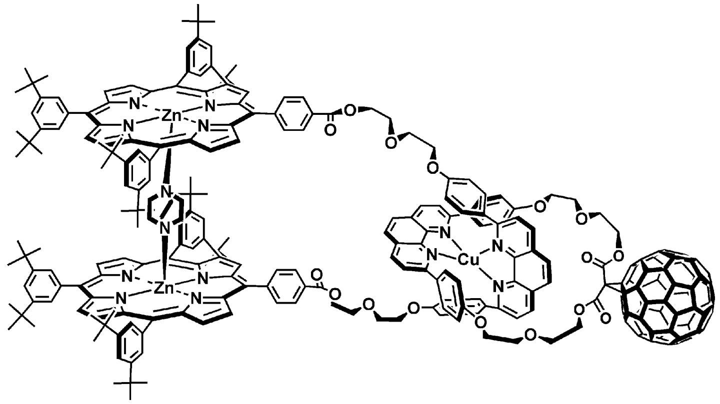

Scheme 11 ZnP-catenane-C_{60} hybrid.

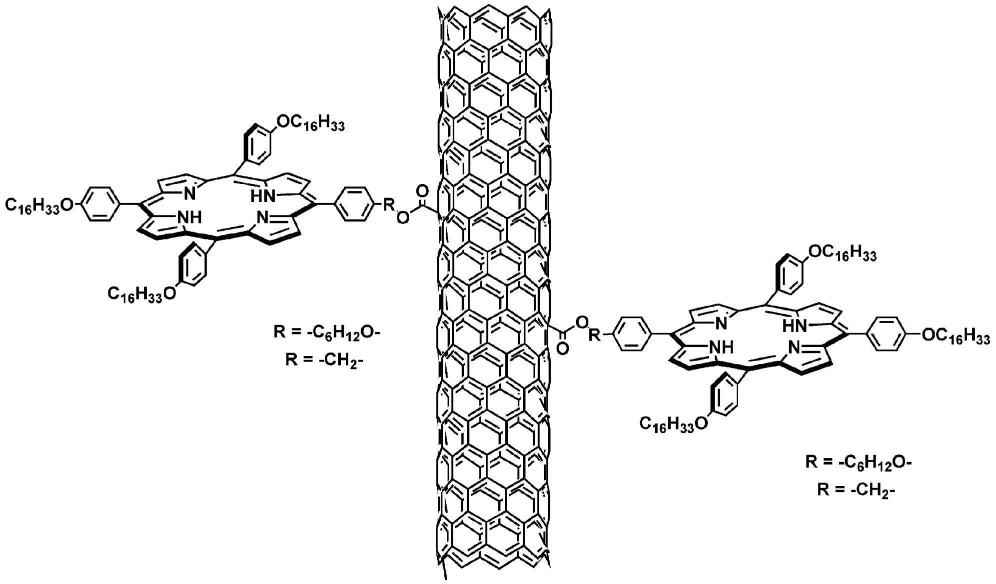

Scheme 12 Covalently linked H_2P-SWNT nanoconjugate.

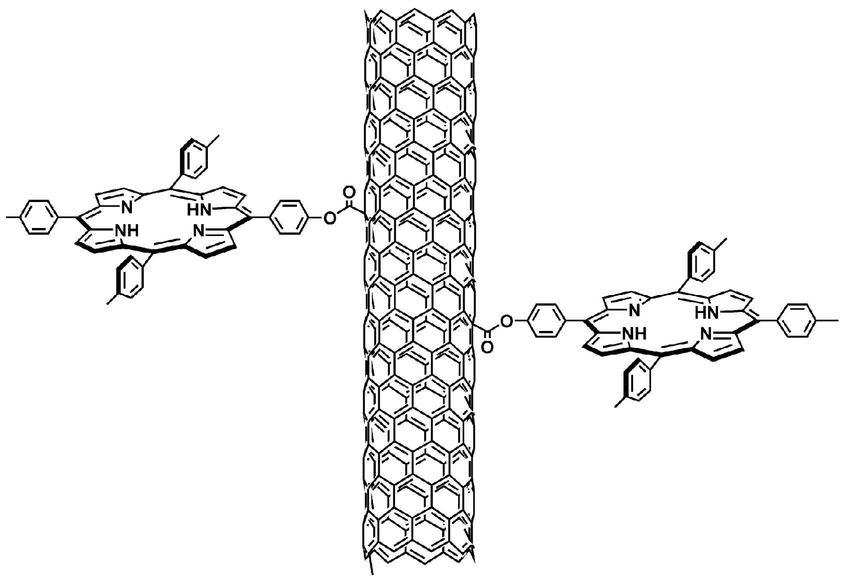

Scheme 13 Covalently linked H_2P-SWNT nanoconjugate.

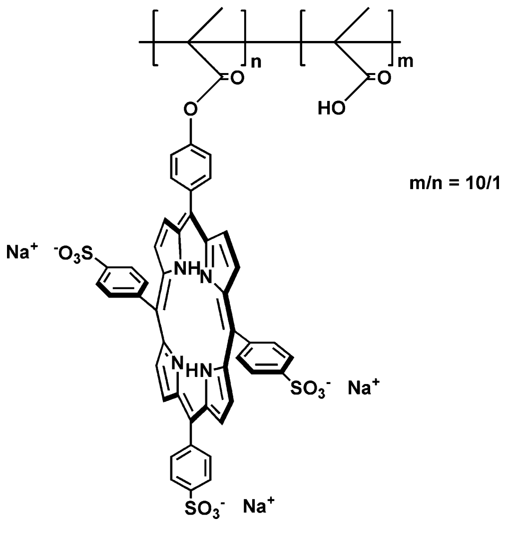

Scheme 14 Partial structure of H_2P-polymer.

for example, the debundling of individual SWNT. An additional feature of H_2P-polymer/SWNT is an intrahybrid charge separation, which has been shown to last for 2.1 ± 0.1 μs.

Stable H_2P/SWNT composites were also realized by condensating tetraformylporphyrins and diaminopyrenes on SWNT.[55] The degree of interaction between SWNT and H_2P was evaluated by UV-vis and fluorescence spectra, and chemical removal of H_2P from SWNT. In the *electron-donor–acceptor* nanohybrids, the Soret and Q-bands of H_2P moieties were significantly broadened and their fluorescence was almost completely quenched. Apparent extinction coefficients at the Soret bands were decreased to *ca.* 20%.

Complementary electrostatics

An important consideration when associating CNT with electron donor building blocks is to preserve—as much as possible—the unique electronic structures of the CNT. A versatile approach involves grafting SWNT with polymers such as poly(sodium 4-styrenesulfonate) (SWNT-PSS^{n-}) with a SWNT to PSS^{n-} ratio of 55/45.[56] In turn, highly stable water dispersable SWNT were prepared with relative ease. The attached PSS functionalities also assist in exfoliating individual SWNT-PSS^{n-} from the larger bundles and stabilizing them. AFM and TEM analysis corroborated the presence of SWNT with lengths reaching several micrometers and diameters around 1.2 nm. A coulomb complex formation was achieved with SWNT-PSS^{n-} and an octapyridinium H_2P salt.[57] Several spectroscopic techniques like absorption, fluorescence, and TEM were used to monitor the complex formation between SWNT-PSS^{n-} and octapyridinium H_2P salt yielding SWNT-PSS^{n-}-electrostatic-H_2P. Importantly, photoexcitation of the octapyridinium H_2P chromophore in the newly formed nanohybrid structure result in efficient intrahybrid charge separation event (0.3 ns), which leads, subsequently, to radical ion pair formation. The charge separation is governed by a large thermodynamic driving force of 0.81 eV. The newly formed radical ion pair exhibits a remarkably long lifetime of 14 μs under anaerobic condition, which constitutes one of longest reported for any CNT ensemble found so far.

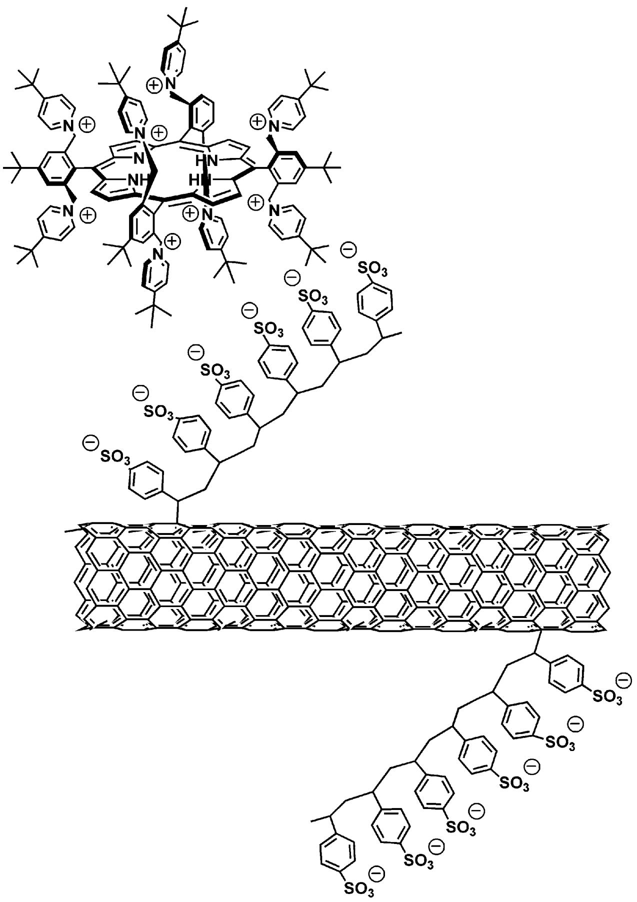

Scheme 15 SWNT-PSS^{n-}-electrostatic-H_2P nanohybrid.

π–π Interactions

An impressive SWNT solubility has been achieved upon treatment with zinc [5,10,15,20-tetraphenyl-21*H*,23*H*-porphine] in DMF.[58] TEM and AFM images revealed the existence of high density SWNT and exfoliation of individual SWNT as a result of the tedious work-up procedure. The CNT diameter ranged typically from 0.9 to 1.5 nm, underlining the successful debundling properties of ZnP. Evidence for interactions between porphyrins and SWNT was obtained from fluorescence spectra, where the porphyrin fluorescence was significantly quenched compared to porphyrin alone. The fluorescence quenching has been ascribed to energy transfer between the photoexcited porphyrin and SWNT.

Similarly, SWNT suspensions in the presence of H_2P—[5,10,15,20-tetrakis(hexadecyloxyphenyl)-21*H*,23*H*-porphine]—in organic solvents yielded novel *electron-donor–acceptor* nanohybrids.[59] Insoluble and recovered SWNT were separated from H_2P by treatment with acetic acid and vigorous centrifugation. After heating the recovered SWNT and the free SWNT to 800 °C in a nitrogen atmosphere, spectroscopic analysis showed that the semiconducting SWNT and the free SWNT are enriched in recovered and metallic SWNT, respectively. Under ambient conditions, the bulk conductivity of semiconducting recovered SWNT is 0.007 S cm^{-1}, while that of metallic free SWNT is 1.1 S cm^{-1}. Thus, selective interactions between H_2P and semiconducting SWNT are the inception to a successful separation of metallic and semiconducting nanotubes.

Water-soluble H_2P [*meso*-(tetrakis-4-sulfonatophenyl) porphine dihydrochloride] was employed to suspend SWNT, resulting in aqueous solutions that are stable for several weeks.[60] These *electron-donor–acceptor* nanohybrids have been characterized by absorption and fluorescence spectroscopy, further complemented by AFM. H_2P and SWNT interact selectively for the free base form, and this interaction stabilizes the free base against protonation to the diacid. Under mildly acidic conditions SWNT mediated J-aggregates form, which are unstable in solution and result in precipitation of the nanotubes over the course of a few days. H_2P coated SWNT can be precisely aligned on hydrophilic poly(dimethylsiloxane) surfaces by combing SWNT solution along a desired direction and then transferred to silicon substrates by stamping.

π–π Interactions and complementary electrostatics

A key requirement to test biological applications and/or biophysical processing is, however, the unlimited dispersability of CNT in aqueous media. With that objective in mind, water-soluble SWNT and MWNT were obtained in aqueous solutions of 1-(trimethylammonium acetyl) pyrene ($pyrene^+$) or 1-pyreneacetic acid, 1-pyrenecarboxylic acid, 1-pyrenebutyric acid, 8-hydroxy-1,3,6-pyrenetrisulfonic acid ($pyrene^-$).[14a,61] Excess free pyrene was removed from solution using vigorous centrifugation and the final CNT-(π–π-interaction)-$pyrene^+$ or CNT-(π–π-interaction)-$pyrene^-$ solids were resuspended in water. The solubility of CNT in the resulting black suspensions is as high as 0.2 mg ml^{-1} and the stability reaches several months under ambient conditions without showing any apparent precipitations. TEM and AFM images revealed the coexistence of individual and bundles of CNT. Now that the surface of CNT is covered with positively or negatively charged ionic head groups, van der Waals and electrostatic interactions are utilized to complex oppositely charged electron donors. Water-soluble porphyrins (*i.e.*, octapyridinium ZnP/H_2P salts or octacarboxylate ZnP/H_2P salts) emerged as ideal candidates to realize SWNT-(π–π-interaction)-$pyrene^+$-electrostatic-ZnP or SWNT-(π–π-interaction)-$pyrene^+$-electrostatic-H_2P *electron-donor–acceptor* nanohybrids.

CNT-(π–π-interaction)-$pyrene^+$-electrostatic-ZnP or CNT-(π–π-interaction)-$pyrene^+$-electrostatic-H_2P were characterized by spectroscopic (absorption and fluorescence) and microscopic (TEM and AFM) means. In absorption experiments, the successful complex formation—for instance, of CNT and ZnP^{8-}—were confirmed by red-shifted Soret- and Q-bands and the development of a series of isosbestic points. Photoexcitation of all the resulting *electron-donor–acceptor* nanohybrids with visible light, causes reduction of the electron accepting CNT and oxidation of the electron donating ZnP or H_2P. In fact, long-lived radical ion pairs—with lifetimes that are in the range of microseconds—were confirmed by transient absorption measurements. It is interesting that a better delocalization of electrons in MWNT helps to significantly enhance the stability of the radical ion pair (5.8 ± 0.2 microseconds) relative to the analogous SWNT (0.4 ± 0.05 microseconds). Percolation of the charge inside the concentric wires in MWNT decelerates the decay dynamics associated with charge recombination.

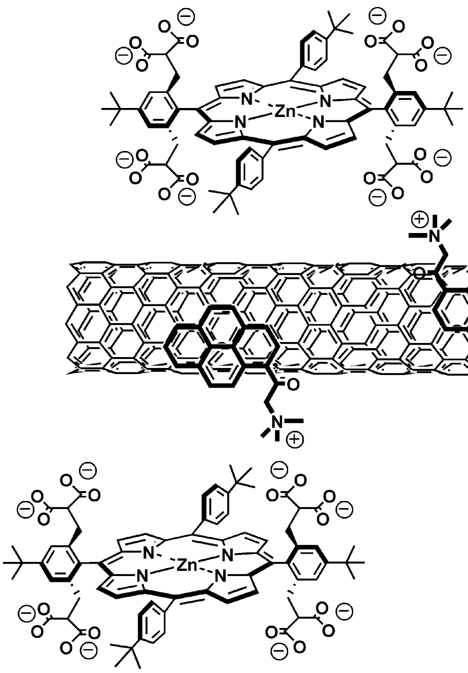

Scheme 16 SWNT-(π–π-interaction)-$pyrene^+$-electrostatic-ZnP nanohybrid.

The pyrene approach towards functional nanohybrids does not form any covalent bonds but only π-π interactions, and perturbs the CNT conjugated system weakly. Pyrene derivatives with a large variety of functional groups can be easily prepared, so that the approach is very general and easy to exploit.

Photoelectrochemical cells—fullerenes and carbon nanotubes

Carbon nanostructures—fullerenes and carbon nanotubes—and porphyrins have been successfully used as integrative components in multifunctional hybrid cells that reveal considerable promise for applications as photochemical energy conversion systems.[62] Please note that sometimes very different photocurrent characterization conditions (*i.e.*, light power, intensities, size of the cells, *etc.*) were used, which limits a meaningful comparison only to photoelectrochemical cell performances that stem from the same laboratories. In the following, a classification of the photoelectrodes is made based on the nature of the support electrode.

Fullerene-porphyrin-gold

Self-assembled monolayers of fullerene-porphyrin systems, is by far the most frequently and systematically studied approach for the construction of nanostructured photoelectrodes. In particular, covalently linked dyad and triad conjugates involving porphyrins and fullerenes with a thiol functionality have been self assembled onto gold electrodes for photocurrent measurements. Cathodic photocurrents were observed upon irradiation of the modified gold electrodes, in which ZnP containing cells revealed better performance than the analogous H_2P cells. Further performance improvements were noted when boron dipyrrin was co-assembled as an antenna—improving the absorption in the green and in the blue region. However, strong excited state quenching of the porphyrin by the gold surface is the limiting factor that prevents attaining higher charge separation quantum yields.[63]

Fullerene-porphyrin-indium tin oxide

Highly transparent (>90%) and conductive (*ca.* $10^4\ \Omega$ cm) indium tin oxide (ITO) support electrodes, are much better suited for nanostructured photoelectrodes than the aforementioned gold electrodes due to the lack of porphyrin singlet excited state quenching. Thiol or siloxy groups were chosen as chemical linkers that help to bind the fullerene-porphyrin conjugates to the electrode surface. Among the fullerene-porphyrin conjugates that bear multiporphyrin arrays/dendrimers H_2P instead of ZnP led to higher photocurrent conversion efficiencies.[64]

More recently, a self-assembled monolayer of ZnP-C_{60} conjugate, in which a triosmium carbonyl cluster moiety links C_{60} and a porphyrin unit and 3-(triethoxysilyl)propyl isocyanide as a surface-anchoring ligand, is shown to exhibit the highest photocurrent efficiency ever reported for a covalently linked systems.[65]

Similarly, non-covalent fullerene-porphyrin hybrids that rely on hydrogen bonding, van der Waals, π–π, and electrostatic interactions have been shown to be suited for the construction of nanostructured photoelectrodes.[66] Most efficient photocurrent generations were accomplished when well tailored energy and redox gradients, in hybrid structures of fullerenes, porphyrins and ferrocenes were constructed.[62a]

Fullerene-porphyrin-indium tin oxide/tin oxide

Adsorbed on nanostructured surfaces of SnO_2—supported on ITO—covalently linked conjugates,[67] and non-covalently hybrids have been characterized in terms of photovoltaic performances. The list of non-covalently hybrids includes hydrogen-bond donor–acceptor supramolecular complexes,[68] supramolecular complexes of porphyrin-peptide oligomers with fullerene,[69] electrodeposited interpenetrated networks of mixed molecular nanoclusters of fullerene and porphyrin,[70] and a quaternary organized gold composite nanoclusters.[71]

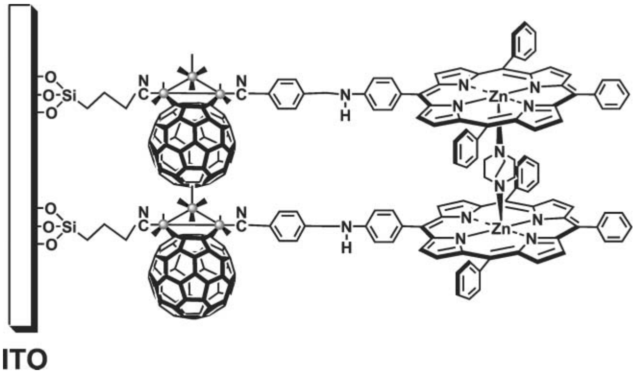

Scheme 17 Photoelectrochemical cell incorporating a self-assembling monolayer of a ZnP-C_{60} conjugate onto ITO.

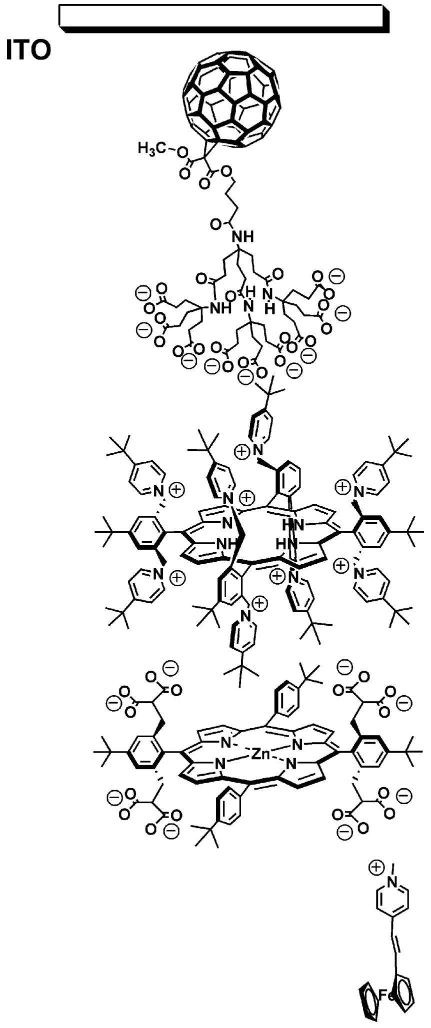

Scheme 18 Photoelectrochemical cell incorporating electrostatically interacting fullerenes, porphyrins and ferrocenes onto ITO that give rise to energy and redox gradients.

The non-covalent hybrid strategy is in general more promising/effective because the photocurrent conversion efficiency has often been limited by the poor vectorial electron flow in covalently linked conjugates.

Carbon nanotube-porphyrin

Some promising first reports on photoelectrochemical devices integrating SWNT—as electron acceptor—on ITO are based on non-covalent assembly strategies.[15d] In most of these instances the ITO electrodes were covered with a base layer of polyelectrolyte (*i.e.*, poly(diallyldimethylammonium)chloride ($PDDA^{n+}$) or sodium polystyrene-4-sulfonate (PSS^{n-})) through hydrophobic–hydrophobic forces. A proper grafting of SWNT with pyrene derivatives, bearing polar functional groups, permits one to disperse them in aqueous media and to assemble them electrostatically to the polyelectrolyte base layer. In the final step, water soluble but oppositely charged porphyrins are assembled as the top layer. This approach has been extended to double wall carbon nanotubes (DWNT), MWNT and thin-MWNT. Importantly, thin-MWNT showed the best performance as electron acceptor layer material.[72]

Summary and outlook

Most *electron-donor–acceptor* ensembles that have been synthesized for probing photoinduced electron transfer processes take advantage of porphyrin derivatives as excited state electron donors and C_{60}/CNT as electron acceptors, due to the remarkable redox and structural features. Several features of these systems retain the characteristics of C_{60} or CNT, which is regarded as one of the key requisites for generating long-lived radical ion pair states.

Sophisticated and well-established methodologies—to functionalize C_{60} covalently and non-covalently—were employed to yield novel and versatile *electron-donor–acceptor* architectures with topologies that include linear structures, tubular structures, rotaxanes, catenanes, *etc*.

In recent years, however, the development of CNT nanoconjugates and nanohybrids has attracted considerable attention. The solubilization of CNT through the use of functional chromophores (*i.e.*, porphyrins) offers outstanding opportunities. In particular, combining the unique electronic properties of SWNT or MWNT with electron donating antennae seems to pave the way to realize a broad range of applications, such as photoelectrochemical/photovoltaic cells, photodiodes, and light-harvesting systems.

One of the major challenges involves the quantitative separation i) of semiconducting and metallic CNT and ii) of different band gap CNT. Diameter, band gap, conductivity and doping might emerge as important variables in the development of efficient solar energy conversion systems.

In the context of photoelectrochemical cells, initial tests with sequentially integrated monolayers of CNT and electron donating porphyrins onto ITO electrodes give rise to promising monochromatic internal photoconversion efficiencies of up to $\sim$10.7%. Although the strategy is by no means optimized, it is a promising starting point that leaves ample room for further improvement.

Finally, the knowledge and database that were established throughout our fundamental studies, focusing on the development of CNT based photovoltaics, is expected to impact other opto-electronic or electro-optic technologies—fuel cells, photocatalysis, sensors, organic thin-film transistors, organic light-emitting diodes, electrochromic materials *etc*.

Acknowledgements

This work was carried out with partial support from the EU (RTN network "WONDERFULL"), SFB 583, DFG (GU 517/4-1), FCI, and the Office of Basic Energy Sciences of the US Department of Energy (NDRL 4654). We are deeply indebted to Profs. Carmichael, Ford, Fukuzumi, Hirsch, Hug, Imahori, Jux, Kotov, Lemmetyinem, Maggini, Martin, Paolucci, Prato, Schuster, Sessler, Tagliatesta, Tkachenko, Torres, Valli, Zerbetto, and Zilbermann for their productive collaborations and numerous stimulating discussions.

In memory of Professor Roger Taylor.

References

1 (*a*) A. F. Collings and C. Critchley, *Artificial Photosynthesis: From Basic Biology to Industrial Application*, Wiley-VCH, Weinheim, (2005); (*b*) V. Balzani, *Electron Transfer in Chemistry*, Wiley-VCH, Weinheim (2001); (*c*) D. M. Guldi, *Chem. Soc. Rev.*, 2002, **31**, 22; (*d*) H. Imahori, Y. Mori and Y. Matano, *J. Photochem. Photobiol., C*, 2003, **4**, 51; (*e*) J. Deisenhofer and J. R. Norris, *The Photosynthetic Reaction Center*; Academic Press: San Diego, (1993); (*f*) D. Gust, T. A. Moore and A. L. Moore, *Acc. Chem. Res.*, 1993, **26**, 198.

2 D. G. Johnson, M. P. Niemczyk, D. W. Minsek, G. P. Wiederrecht, W. A. Svec, G. L. Gaines and M. R. Wasielewski, *J. Am. Chem. Soc.*, 1993, **115**, 5692.

3 (*a*) D. M. Guldi, *Pure Appl. Chem.*, 2003, **75**, 1069; (*b*) D. M. Guldi, *Spectrum*, 2003, **16**, 23.

4 (*a*) D. J. Lakhno Victor, *Biol. Phys.*, 2005, **31**, 145; (*b*) M. Marchi, J. N. Gehlen, D. Chandler and M. Newton, *J. Am. Chem. Soc.*, 1993, **115**, 4178.

5 D. M. Guldi and S. Fukuzumi, *Dev. Fullerene Sci.*, 2002, **4**, 237.

6 (*a*) W. Fritzsche and M. Köhler, *Nanotechnology: An Introduction to Nanostructuring Techniques*, Wiley-VCH, Weinheim, Germany, (2004); (*b*) C. Rao, *Chemistry of Nanomaterials: Synthesis, Properties and Applications*, Wiley-VCH, Weinheim, Germany, (2004); (*c*) E. Wolf, *Nanophysics and Nanotechnology: An Introduction to Modern Concepts in Nanoscience*, Wiley-VCH, Weinheim, Germany, (2004); (*d*) G. Cao, *Nanostructures and Nanomaterials: Synthesis, Properties & Applications*, Imperial College Press, London, (2004).

7 (*a*) A. Hirsch and M. Brettreich, *Fullerenes: Chemistry and Reactions*, Wiley-VCH, Weinheim, (2004); (*b*) K. M. Kadish and R. S. Ruoff, *Fullerenes: Chemistry, Physics, and Technology*, Wiley-VCH, Weinheim, (2000); (*c*) D. M. Guldi and N. Martin, *Fullerenes: From Synthesis to Optoelectronic Properties*, Series: *Developments in Fullerene Science*, Kluwer Academic, Dordrecht, (2002); (*d*) T. Braun, *Nuclear and Radiation Chemical Approaches to Fullerene Science,* Series: *Developments in Fullerene Science*,**Vol. 1,** Kluwer Academic, Dordrecht, (2000).

8 (*a*) F. Diederich, L. Isaacs and D. Philp, *Chem. Soc. Rev.*, 1994, **23**, 243; (*b*) M. Prato and M. Maggini, *Acc. Chem. Res.*, 1998, **31**, 519; (*c*) D. Tasis, N. Tagmatarchis, V. Georgakilas, C. Gamboz, M.-R. Soranzo and M. Prato, *C. R. Chim.*, 2003, **6**, 597; (*d*) N. Tagmatarchis and M. Prato, *Synlett*, 2003, **6**, 768; (*e*) F. Diederich and M. Gomez-Lopez, *Chem. Soc. Rev.*, 1999, **28**, 263.

9 (*a*) S. Reich, C. Thomsen and J. Maultzsch, *Carbon Nanotubes: Basic concepts and Physical Properties*, Wiley-VCH, Weinheim, Germany, (2004); (*b*) M. S. Dresselhaus, G. Dresselhaus and P. Avouris, *Carbon Nanotubes: Synthesis, Structure, Properties and Applications*, Springer, Berlin, (2001); (*c*) P. J. F. Harris, *Carbon Nanotubes and Related Structures: New Materials for the Twenty-First Century*, Cambridge University Press, Cambridge, UK, (2001); (*d*) Special issue on Carbon Nanotubes, *Acc. Chem. Res.*, 2002, **35**, 997; (*e*) S. Roth and D. Carroll, *One-Dimensional Metals: Conjugated Polymers, Organic Crystals, Carbon Nanotubes*, Wiley-VCH, Weinheim, Germany, 2004.

10 (*a*) M. F. Yu, B. S. Files, S. Arepalli and R. S. Ruoff, *Phys. Rev. Lett.*, 2000, **84**, 5552; (*b*) S. Ijima, C. Brabec, A. Maiti and J. Bernholc, *J. Chem. Phys.*, 1996, **104**, 2089; (*c*) M. M. J. Treacy, T. W. Ebbesen and J. M. Gibson, *Nature*, 1996, **381**, 678; (*d*) M. R. Falvo, G. J. Clary, R. M. Taylor, V. Chi, F. P. Brooks, S. Washburn and R. Superfine, *Nature*, 1997, **389**, 582; (*e*) P. A. Calvert, *Nature*, 1999, **399**, 210.

11 (*a*) S. T. Huxtable, D. G. Cahill, S. Shenogin, L. Xue, R. Ozisik, P. Barone, M. Usrey, M. S. Strano, G. Siddons, M. Shim and P. Keblinski, *Nat. Mat.*, 2003, **2**, 731; (*b*) H. L. Zhang, J. F. Li, K. F. Yao and L. D. Chen, *J. Appl. Phys.*, 2005, **97**, 114310; (*c*) N. Mingo and D. A. Broido, *Nano Lett.*, 2005, **5**, 1221; (*d*) Y. Sun, T. Miyasato, K. Kirimoto and M. Kusunoki, *Appl. Phys. Lett.*,

2005, **86**, 223108/1; (*e*) P. Kim, L. Shi, A. Majumdar and P. L. McEuen, *Phys. Rev. Lett.*, 2001, **87**, 215502; (*f*) J. Hone, B. Batlogg, Z. Benes, A. T. Johnson and J. E. Fischer, *Science*, 2000, **289**, 1730.

12 (*a*) J. A. Misewich, P. Avouris, R. Martel, J. C. Tsang, S. Heinz and J. Tersoff, *Science*, 2003, **300**, 783; (*b*) N. De Jonge, M. Allioux, M. Doytcheva, M. Kaiser, K. B. K. Teo, R. G. Lacerda and W. I. Milne, *Appl. Phys. Lett.*, 2004, **85**, 1607; (*c*) S. H. Jo, D. Z. Wang, J. Y. Huang, W. Z. Li, K. Kempa and Z. F. Ren, *Appl. Phys. Lett.*, 2004, **85**, 810; (*d*) S. M. Yoon, J. Chae and J. S. Suh, *Appl. Phys. Lett.*, 2004, **84**, 825; (*e*) A. Buldum and J. P. Lu, *Phys. Rev. Lett.*, 2003, **91**, 236801/1.

13 (*a*) X. L. Liang, L.-M. Peng, Q. Chen, R. C. Che, Y. Xia, Z. Q. Xue and Q. D. Wu, *Phys. Rev. B: Condens. Matter Mater. Phys.*, 2003, **68**, 073403/1; (*b*) P. G. Collins, M. S. Arnold and P. Avouris, *Science*, 2001, **292**, 706.

14 (*a*) D. M. Guldi, G. M. A. Rahman, N. Jux, D. Balbinot, N. Tagmatarchis and M. Prato, *Chem. Commun.*, 2005, 2038; (*b*) W. Feng, A. Fujii, M. Ozaki and K. Yoshino, *Carbon*, 2005, **43**, 2501.

15 (*a*) G. M. A. Rahman, D. M. Guldi, R. Cagnoli, A. Mucci, L. Schenetti, L. Vaccari and M. Prato, *J. Am. Chem. Soc.*, 2005, **127**, 10051; (*b*) B. J. Landi, S. L. Castro, H. J. Ruf, C. M. Evans, S. G. Bailey and R. P. Raffaelle, *Sol. Energy Mater. Sol. Cells*, 2005, **87**, 733; (*c*) K.-I. Nakayama, Y. Asakura and M. Yokoyama, *Mol. Cryst. Liq. Cryst.*, 2004, **424**, 217; (*d*) D. M. Guldi, G. M. A. Rahman, M. Prato, N. Jux, S. Qin and W. Ford, *Angew. Chem., Int. Ed.*, 2005, **44**, 2015; (*e*) B. J. Landi, R. P. Raffaelle, S. L. Castro and S. G. Bailey, *Prog. Photovoltaics*, 2005, **13**, 165; (*f*) J. A. Rud, L. S. Lovell, J. W. Senn, Q. Qiao and J. T. Mcleskey, *J. Mat. Sci.*, 2005, **40**, 1455; (*g*) S.-R. Jang, R. Vittal and K.-J. Kim, *Langmuir*, 2004, **20**, 9807; (*h*) E. Kymakis and G. A. J. Amaratunga, *Sol. Energy Mater. Sol. Cells*, 2003, **80**, 465; (*i*) K.-H. Jung, J. S. Hong, R. Vittal and K.-J. Kim, *Chem. Lett.*, 2002, **8**, 864; (*j*) E. Kymakis and G. A. J. Amaratunga, *Appl. Phys. Lett.*, 2002, **80**, 112.

16 (*a*) D. Tasis, N. Tagmatarchis, V. Georgakilas and M. Prato, *Chem.–Eur. J.*, 2003, **9**, 4000; (*b*) C. A. Dyke and J. M. Tour, *Chem.–Eur. J.*, 2004, **10**, 812; (*c*) A. Ikeda, K. Hayashi, T. Konishi and J.-I. Kikuchi, *Chem. Commun.*, 2004, 1334; (*d*) K. Shen, S. Curran, H. Xu, S. Rogelj, Y. Jiang, J. Dewald and T. Pietrass, *J. Phys. Chem. B*, 2005, **109**, 4455; (*e*) N. Grossiord, O. Regev, J. Loos, J. Meuldijk and C. E. Koning, *Anal. Chem.*, 2005, **77**, 5135; (*f*) M. Melle-Franco, M. Marcaccio, D. Paolucci, F. Paolucci, V. Georgakilas, D. M. Guldi, M. Prato and F. Zerbetto, *J. Am. Chem. Soc.*, 2004, **126**, 1646; (*g*) D. M. Guldi, M. Holzinger, A. Hirsch, V. Georgakilas and M. Prato, *Chem. Commun.*, 2003, 1130.

17 (*a*) J. Li, Y. Zhang and M. Zhang, *Chem. Phys. Lett.*, 2002, **364**, 328; (*b*) M. Yoshida and J.-I. Aihara, *Phys. Chem. Chem. Phys.*, 1999, **1**, 227; (*c*) J.-I. Aihara and H. Kanno, *Chem. Phys. Lett.*, 2004, **398**, 440.

18 (*a*) K. Kalyanasundaram, *Photochemistry of Polypyridine and Porphyrin Complexes*, Academic Press, London, (1997); (*b*) M. Gouterman, P. M. Rentzepis and K. D. Straub, *Porphyrins: Excited States and Dynamics*, ACS Symposium Series, N° 321, (1987); (*c*) D. Dolphin, *The Porphyrins*, Academic Press, New York, (1978); (*d*) K. M. Kadish, K. M. Smith and R. Guilard, *The Porphyrin Handbook*, Academic Press, New York, (2003).

19 (*a*) R. A. Marcus, *J. Chem. Phys.*, 1956, **24**, 966; (*b*) R. Marcus and N. Sutin, *Biophys. Acta*, 1985, **811**, 265; (*c*) R. A. Marcus, *Angew. Chem., Int. Ed. Engl.*, 1993, **32**, 1111.

20 V. Gladkikh, A. I. Burshtein, G. Angulo, S. Pages, B. Lang and E. Vauthey, *J. Phys. Chem. A*, 2004, **108**, 6667.

21 H. Imahori, H. Yamada, D. M. Guldi, Y. Endo, A. Shimomura, S. Kundu, K. Yamada, T. Okada, Y. Sakata and S. Fukuzumi, *Angew. Chem., Int. Ed.*, 2002, **41**, 2344.

22 (*a*) H. Imahori, K. Tamaki, H. Yamada, K. Yamada, Y. Sakata, Y. Nishimura, I. Yamazaki, M. Fujitsuka and O. Ito, *Carbon*, 2000, **38**, 1599; (*b*) H. Imahori, K. Hagiwara, T. Akiyama, M. Aoki, S. Taniguchi, T. Okada, M. Shirakawa and Y. Sakata, *Chem. Phys. Lett.*, 1996, **263**, 545.

23 (*a*) L. Hviid, J. W. Verhoeven, A. M. Brouwer, M. N. Paddon-Row and Jixin Yang, *Photochem. Photobiol. Sci.*, 2004, **3**, 246; (*b*) M. Bixon and J. Jortner, *J. Chem. Phys.*, 1997, **107**, 5154; (*c*) D. M. Guldi, M. Maggini, N. Martin and M. Prato, *Carbon*, 2000, **38**, 1615.

24 (*a*) D. I. Schuster, P. Cheng, P. D. Jarowski, D. M. Guldi, C. Luo, L. Echegoyen, S. Pyo, A. R. Holzwarth, S. E. Braslavsky, R. M. Williams and G. Klihm, *J. Am. Chem. Soc.*, 2004, **126**, 7257; (*b*) T. Galili, A. Regev, H. Levanon, D. I. Schuster and D. M. Guldi, *J. Phys. Chem. A*, 2004, **108**, 10632; (*c*) E. Sim, *J. Phys. Chem. B*, 2005, **109**, 11829.

25 (*a*) M. N. Paddon-Row, *Aust. J. Chem.*, 2003, **56**, 729; (*b*) E. G. Petrov and V. May, *J. Phys. Chem. A*, 2001, **105**, 10176; (*c*) E. G. Petrov, Y. V. Shevchenko, V. I. Teslenko and V. May, *J. Chem. Phys.*, 2001, **115**, 7107; (*d*) H. Sumi and T. Kakitani, *J. Phys. Chem. B*, 2001, **105**, 9603; (*e*) I. R. Gould, R. H. Young, L. J. Mueller and S. Farid, *J. Am. Chem. Soc.*, 1994, **116**, 8176; (*f*) H. Guo, L. Liu and K. Lao, *Chem. Phys. Lett.*, 1994, **218**, 212; (*g*) J. Tang, Z. Wang and J. R. Norris, *J. Chem. Phys.*, 1993, **99**, 979; (*h*) B. P. Paulson, J. R. Miller, W.-X. Gan and G. Closs, *J. Am. Chem. Soc.*, 2005, **127**, 4860.

26 (*a*) H. Imahori, D. M. Guldi, K. Tamaki, Y. Yoshida, C. Luo, Y. Sakata and S. Fukuzumi, *J. Am. Chem. Soc.*, 2001, **123**, 6617; (*b*) D. M. Guldi, H. Imahori, K. Tamaki, Y. Kashiwagi, H. Yamada, Y. Sakata and S. Fukuzumi, *J. Phys. Chem. A*, 2004, **108**, 541; (*c*) C. Luo, D. M. Guldi, H. Imahori, K. Tamaki and Y. Sakata, *J. Am. Chem. Soc.*, 2000, **122**, 6535.

27 (*a*) A. Osuka, K. Maruyama, N. Mataga, T. Asahi, I. Yamazaki and N. Tamai, *J. Am. Chem. Soc.*, 1990, **112**, 4958; (*b*) S. Speiser, *Chem. Rev.*, 1996, **96**, 1953; (*c*) S. B. Sachs, S. P. Dudek, R.P. Hsung, L. R. Sita, J. F. Smalley, M. D. Newton, S. W. Feldberg and C. E. D. Chidsey, *J. Am. Chem. Soc.*, 1997, **119**, 10563; (*d*) A. C. Benniston, V. Goulle, A. Harriman, J. M. Lehn and B. Marczinke, *J. Phys. Chem.*, 1994, **98**, 7798.

28 (*a*) E. A. Weiss, M. J. Ahrens, L. E. Sinks, A. V. Gusev, M. A. Ratner and M. R. Wasielewski, *J. Am. Chem. Soc.*, 2004, **126**, 5577; (*b*) A. Nitzan and M. A. Ratner, *Science*, 2003, **300**, 1384; (*c*) W. B. Davis, W. A. Svec, M. A. Ratner and M. R. Wasielewski, *Nature*, 1998, **396**, 60; (*d*) N. Robertson and C. A. McGowan, *Chem. Soc. Rev.*, 2003, **32**, 96; (*e*) K. Balasubramanian, M. Burghard, K. Kern, M. Scolari and A. Mews, *Nano Lett.*, 2005, **5**, 507.

29 F. Giacalone, J. L. Segura, N. Martin, J. Ramey and D. M. Guldi, *Chem.–Eur. J.*, 2005, **11**, 4819.

30 S. A. Vail, P. J. Krawczuk, D. M. Guldi, A. Palkar, L. Echegoyen, J. P. C. Tome, M. A. Fazio and D. I. Schuster, *Chem.–Eur. J.*, 2005, **11**, 3375.

31 (*a*) E. Diez-Barra, J. C. Garcia-Martinez, R. del Rey, J. Rodriguez-Lopez, F. Giacalone, J. L. Segura and N. Martin, *J. Org. Chem.*, 2003, **68**, 3178; (*b*) H. Higuchi, E. Ohta, H. Kawai, K. Fujiwara, T. Tsuji and T. Suzuki, *J. Org. Chem.*, 2003, **68**, 6605; (*c*) R. Gomez, J. L. Segura and N. Martin, *J. Org. Chem.*, 2000, **65**, 7566.

32 D. M. Guldi, F. Giacalone, G. de la Torre, J. L. Segura and N. Martín, *Chem.–Eur. J.*, 2005, **11**, 7199.

33 T. Nakamura, J. Ikemoto, M. Fujitsuka, Y. Araki, O. Ito, K. Takimiya, Y. Aso and T. Otsubo, *J. Phys. Chem. B*, 2005, **109**, 14365.

34 (*a*) T. Da Ros, M. Prato, D. M. Guldi, M. Ruzzi and L. Pasimeni, *Chem.–Eur. J.*, 2001, **7**, 816; (*b*) D. M. Guldi, B. Nuber, P. J. Bracher, C. A. Alabi, S. MacMahon, J. W. Kukol, S. R. Wilson and D. I. Schuster, *J. Phys. Chem. A*, 2003, **107**, 3215.

35 D. M. Guldi, T. Da Ros, P. Braiuca and M. Prato, *Photochem. Photobiol. Sci.*, 2003, **2**, 1067.

36 L. R. Sutton, M. Scheloske, K. S. Pirner, A. Hirsch, D. M. Guldi and J.-P. Gisselbrecht, *J. Am. Chem. Soc.*, 2004, **126**, 10370.

37 Unpublished results.

38 (*a*) J. L. Sessler, J. Jayawickramarajah, A. Gouloumis, T. Torres, D. M. Guldi, S. Maldonado and K. J.Stevenson, *Chem. Commun.*, 2005, **14**, 1892; (*b*) L. Sanchez, N. Martin and D. M. Guldi, *Angew. Chem., Int. Ed.*, 2005, **44**, 5374; (*c*) J. L. Sessler, J. Jayawickramarajah, A. Gouloumis, G. Dan Pantos, T. Torres and D. M. Guldi, *Tetrahedron*, 2006, **62**, 2123.

39 (*a*) F. Marotti, D. Bonifazi, R. Gehrig, J.-L. Gallani and F. Diederich, *Isr. J. Chem.*, 2005, **45**, 303; (*b*) N. Solladie, M. E. Walther, M. Gross, T. M. Figueira Duarte, C. Bourgogne and J.-F. Nierengarten, *Chem. Commun.*, 2003, 2412.

40 D. Balbinot, S. Atalick, D. M. Guldi, M. Hatzimarinaki, A. Hirsch and N. Jux, *J. Phys. Chem. B*, 2003, **107**, 13273.
41 (*a*) I. Zilbermann, A. Lin, M. Hatzimarinaki, A. Hirsch and D. M. Guldi, *Chem. Commun.*, 2004, 96; (*b*) M. Braun, S. Atalick, D. M. Guldi, H. Lanig, M. Brettreich, S. Burghardt, M. Hatzimarinaki, E. Ravanelli, M. Prato, R. van Eldik and A. Hirsch, *Chem.–Eur. J.*, 2003, **9**, 3867.
42 (*a*) D. M. Guldi, A. Gouloumis, P. Vázquez, T. Torres, V. Georgakilas and M. Prato, *J. Am. Chem. Soc.*, 2005, **127**, 5811; (*b*) V. Georgakilas, F. Pellarini, M. Prato, D. M. Guldi, L. Troisi, M. Melle-Franco and F. Zerbetto, *Proc. Natl. Acad. Sci. U. S. A.*, 2002, **99**, 5075.
43 F. D'Souza and O. Ito, *Coord. Chem. Rev.*, 2005, **29**, 1410.
44 F. Hauke, A. Swartz, D. M. Guldi and A. Hirsch, *J. Mater. Chem.*, 2002, **12**, 2088.
45 (*a*) S. R. Wilson, S. MacMahon, F. T. Tat, P. D. Jarowski and D. I. Schuster, *Chem. Commun.*, 2003, 226; (*b*) T. Galili, A. Regev, A. Berg, H. Levanon, D. I. Schuster, K. Mobius and A. Savitsky, *J. Phys. Chem. B*, 2005, **109**, 8451.
46 D. M. Guldi and N. Martin, *J. Mater. Chem.*, 2002, **12**, 1978.
47 (*a*) J.-P. Sauvage and C. O.-Dietrich Buchecker, *Molecular Catenanes, Rotaxanes and Knots*; Wiley-VCH, Weinheim, (1999); (*b*) C. O. Dietrich-Buchecker and J.-P. Sauvage, *Chem. Rev.*, 1987, **87**, 795; (*c*) D. B. Amabilino and J. F. Stoddart, *Chem. Rev.*, 1995, **95**, 2725; (*d*) R. Jager and F. Vogtle, *Angew. Chem., Int. Ed. Engl.*, 1997, **36**, 930.
48 (*a*) K. Li, D. I. Schuster, D. M. Guldi, M. A. Herranz and L. Echegoyen, *J. Am. Chem. Soc.*, 2004, **126**, 3388; (*b*) K. Li, P. J. Bracher, D. M. Guldi, M. A. Herranz, L. Echegoyen and D. I. Schuster, *J. Am. Chem. Soc.*, 2004, **126**, 9156; (*c*) D. I. Schuster, K. Li and D. M. Guldi, *C. R. Chim.*, 2005, 00000.
49 D. I. Schuster, K. Li, D. M. Guldi and J. Ramey, *Org. Lett.*, 2004, **6**, 1919.
50 A. S. D. Sandanayaka, N. Watanabe, K. I. Ikeshita, Y. Araki, N. Kihara, Y. Furusho, O. Ito and T. Takata, *J. Phys. Chem. B*, 2005, **109**, 2516.
51 (*a*) S. Banerjee, T. Hemraj-Benny and S. S. Wong, *Adv. Mater.*, 2005, **17**, 17; (*b*) J. Chen, M. A. Hamon, H. Hu, Y. S. Chen, A. M. Rao, P. C. Eklund and R. C. Haddon, *Science*, 1998, **282**, 95; (*c*) V. Georgakilas, D. Voulgaris, E. Vazquez, M. Prato, D. M. Guldi, A. Kukovecz and H. Kuzmany, *J. Am. Chem. Soc.*, 2002, **124**, 14318; (*d*) J. L. Bahr, D. V. Kosynkin, M. J. Bronikowski, R. E. Smalley and J. M. Tour, *J. Am. Chem. Soc.*, 2001, **123**, 6536; (*e*) C. A. Dyke and J. M. Tour, *J. Am. Chem. Soc.*, 2003, **125**, 1156; (*f*) S. Pekker, J. P. Salvetat, E. Jakab, J. M. Bonard and L. Forro, *J. Phys. Chem. B*, 2001, **105**, 7938; (*g*) M. Holzinger, O. Vostrowsky, A. Hirsch, F. Hennrich, M. Kappes, R. Weiss and F. Jellen, *Angew. Chem., Int. Ed.*, 2001, **40**, 4002; (*h*) Y. Ying, R. K. Saini, F. Liang, A. K. Sadana and W. E. Billups, *Org. Lett.*, 2003, **5**, 1471; (*i*) V. Georgakilas, K. Kordatos, M. Prato, D. M. Guldi, M. Holzinger and A. Hirsch, *J. Am. Chem. Soc.*, 2002, **124**, 760; (*j*) X. D. Lou, R. Daussin, S. Cuenot, A. S. Duwez, C. Pagnoulle, C. Detrembleur, C. Bailly and R. Jerome, *Chem. Mater.*, 2004, **16**, 4005.
52 H. Li, R. B. Martin, B. A. Harruff, R. A. Carino, L. F. Allard and Y.-P. Sun, *Adv. Mater.*, 2004, **16**, 896.
53 D. Baskaran, J. W. Ways, X. P. Zhang and M. S. Bratcher, *J. Am. Chem. Soc.*, 2005, **127**, 6916.
54 D. M. Guldi, H. Taieb, G. M. A. Rahman, N. Tagmatarchis and M. Prato, *Adv. Mater.*, 2005, **17**, 871.
55 A. Satake, Y. Miyajima and Y. Kobuke, *Chem. Mater.*, 2005, **17**, 716.
56 S. Qin, D. Qin, W. T. Ford, J. E. Herrera, D. E. Resasco, S. M. Bachilo and R. B. Weisman, *Macromolecules*, 2004, **35**, 3965.
57 D. M. Guldi, G. M. A. Rahman, J. Ramey, M. Marcaccio, D. Paolucci, F. Paolucci, S. Qin, W. T. Ford, D. Balbinot, N. Jux, N. Tagmatarchis and M. Prato, *Chem. Commun.*, 2004, 2034.
58 H. Murakami, T. Nomura and N. Nakashima, *Chem. Phys. Lett.*, 2003, **378**, 481.
59 H. Li, B. Zhou, Y. Lin, L. Gu, W. Wang, K. A. S. Fernando, S. Kumar, L. F. Allard and Y.-P. Sun, *J. Am. Chem. Soc.*, 2004, **126**, 1014.
60 J. Chen and C. P. Collier, *J. Phys. Chem. B*, 2005, **109**, 7605.
61 (*a*) D. M. Guldi and M. Prato, *Chem. Commun.*, 2004, 2517; (*b*) D. M. Guldi, G. M. A. Rahman, N. Jux, D. Balbinot, U. Hartnagel, N. Tagmatarchis and M. Prato, *J. Am. Chem. Soc.*, 2005, **127**, 9830; (*c*) D. M. Guldi, G. M. A. Rahman, V. Sgobba, S. Campidelli, M. Prato and N. A. Kotov, *J. Am. Chem. Soc.*, 2006, **128**, 2315.
62 (*a*) D. M. Guldi, *J. Phys. Chem. B*, 2005, **109**, 11432; (*b*) H. Imahori, Y. Mori and Y. Matano, *J. Photochem. Photobiol., C*, 2003, **4**, 51; (*c*) H. Imahori, *Org. Biomol. Chem.*, 2004, **2**, 1425; (*d*) H. Imahori and S. Fukuzumi, *Adv. Mater.*, 2004, **14**, 525.
63 (*a*) H. Imahori, H. Yamada, S. Ozawa, K. Ushida and Y. Sakata, *Chem. Commun.*, 1999, 1165; (*b*) H. Imahori, H. Norieda, H. Yamada, Y. Nishimura, I. Yamazaki, Y. Sakata and S. Fukuzumi, *J. Am. Chem. Soc.*, 2001, **123**, 100; (*c*) H. Yamada, H. Imahori and S. Fukuzumi, *J. Mater. Chem.*, 2002, **12**, 2034.
64 (*a*) H. Yamada, H. Imahori, Y. Nishimura, I. Yamazaki and S. Fukuzumi, *Adv. Mater.*, 2002, **14**, 892; (*b*) V. Chukharev, T. Vuorinen, A. Efimov, N. V. Tkachenko, M. Kimura, S. Fukuzumi, H. Imahori and H. Lemmetyinen, *Langmuir*, 2005, **21**, 6385; (*c*) H. Yamada, H. Imahori, Y. Nishimura, I. Yamazaki, T. K. Ahn, S. K. Kim, D. Kim and S. Fukuzumi, *J. Am. Chem. Soc.*, 2003, **125**, 9129; (*d*) H. Imahori, M. Kimura, K. Hosomizu, T. Sato, T. K. Ahn, S. K. Kim, D. Kim, Y. Nishimura, I. Yamazaki, Y. Araki, O. Ito and S. Fukuzumi, *Chem.–Eur. J.*, 2004, **10**, 5111; (*e*) H. Yamada, H. Imahori, Y. Nishimura, I. Yamazaki, T. K. Ahn, S. K. Kim, D. Kim and S. Fukuzumi, *J. Am. Chem. Soc.*, 2003, **125**, 9129; (*f*) H. Imahori, *J. Phys. Chem. B*, 2004, **108**, 6130.
65 Y. J. Cho, T. K. Ahn, H. Song, K. S. Kim, C. Y. Lee, W. S. Seo, K. Lee, S. K. Kim, D. Kim and J. T. Park, *J. Am. Chem. Soc.*, 2005, **127**, 2380.
66 (*a*) H. Imahori, J.-C. Liu, K. Hosomizu, T. Sato, Y. Mori, H. Hotta, Y. Matano, Y. Araki, O. Ito, N. Maruyama and S. Fujita, *Chem. Commun.*, 2004, 2066; (*b*) D. M. Guldi, I. Zilbermann, G. A. Anderson, K. Kordatos, M. Prato, R. Tafuro and L. Valli, *J. Mater. Chem.*, 2004, **14**, 303; (*c*) S. Conoci, D. M. Guldi, S. Nardis, R. Paolesse, K. Kordatos, M. Prato, G. Ricciardi, M. G. H. Vicente, I. Zilbermann and L. Valli, *Chem.–Eur. J.*, 2004, **10**, 6523; (*d*) T. Vuorinen, K. Kaunisto, N. V. Tkachenko, A. Efimov, H. Lemmetyinen, A. S. Alekseev, K. Hosomizu and H. Imahori, *Langmuir*, 2005, **21**, 5383; (*e*) D. M. Guldi, I. Zilbermann, G. Anderson, A. Li, D. Balbinot, N. Jux, M. Hatzimarinaki, A. Hirsch and M. Prato, *Chem. Commun.*, 2004, 726; (*f*) D. M. Guldi, F. Pellarini, M. Prato, C. Granito and L. Troisi, *Nano Lett.*, 2002, **2**, 965.
67 M. E. Milanesio, M. Gervaldo, L. A. Otero, L. Sereno, J. J. Silber and E. N. Durantini, *J. Phys. Org. Chem.*, 2002, **15**, 844.
68 H. Imahori, J. C. Liu, H. Hotta, A. Kira, T. Umeyama, Y. Matano, G. Li, S. Ye, M. Isosomppi, N. V. Tkachenko and H. Lemmetyinen, *J. Phys. Chem. B*, 2005, **109**, 18465.
69 T. Hasobe, P. V. Kamat, V. Troiani, N. Solladié, T. K. Ahn, S. K. Kim, D. Kim, A. Kongkanand, S. Kuwabata and S. Fukuzumi, *J. Phys. Chem. B*, 2005, **109**, 19.
70 (*a*) T. Hasobe, H. Imahori, S. Fukuzumi and P. V. Kamat, *J. Phys. Chem. B*, 2003, **107**, 12105; (*b*) T. Hasobe, P. V. Kamat, M. A. Absalom, Y. Kashiwagi, J. Sly, M. J. Crossley, K. Hosomizu, H. Imahori and S. Fukuzumi, *J. Phys. Chem. B*, 2004, **108**, 12865; (*c*) T. Hasobe, Y. Kashiwagi, M. A. Absalom, J. Sly, K. Hosomizu, M. J. Crossley, H. Imahori, P. V. Kamat and S. Fukuzumi, *Adv. Mater.*, 2004, **16**, 975; (*d*) H. Imahori, T. Hasobe, H. Yamada, P. V. Kamat, S. Barazzouk, M. Fujitsuka, O. Ito and S. Fukuzumi, *Chem. Lett.*, 2001, **8**, 784.
71 (*a*) T. Hasobe, H. Imahori, P. V. Kamat and S. Fukuzumi, *J. Am. Chem. Soc.*, 2003, **125**, 14962; (*b*) H. Imahori, A. Fujimoto, S. Kang, H. Hotta, K. Yoshida, T. Umeyama, Y. Matano and S. Isoda, *Adv. Mater.*, 2005, **17**, 1727; (*c*) T. Hasobe, H. Imahori, P. V. Kamat, T. K. Ahn, S. K. Kim, D. Kim, A. Fujimoto, T. Hirakawa and S. Fukuzumi, *J. Am. Chem. Soc.*, 2005, **127**, 1216.
72 D. M. Guldi, G. M. A. Rahman, V. Sgobba, S. Campidelli and M. Prato, *Adv. Mat.* submitted.